European Journal of Medicinal Chemistry 218 (2021) 113352

Contents lists available at ScienceDirect

European Journal of Medicinal Chemistry

journal homepage: http://www.elsevier.com/locate/ejmech

Insertion of metal carbenes into the anilinic *N*—*H* bond of unprotected aminobenzenesulfonamides delivers low nanomolar inhibitors of human carbonic anhydrase IX and XII isoforms

Tatiana Sharonova [a], Polina Paramonova [a], Stanislav Kalinin [a], Alexander Bunev [b], Rovshan E. Gasanov [b], Alessio Nocentini [c], Vladimir Sharoyko [a], Tatiana B. Tennikova [a], Dmitry Dar'in [a], Claudiu T. Supuran [c, **], Mikhail Krasavin [a, *]

[a] Saint Petersburg State University, Saint Petersburg, 199034, Russian Federation
[b] Medicinal Chemistry Center, Togliatti State University, Togliatti, 445020, Russian Federation
[c] Neurofarba Department, Universita degli Studi di Firenze, Florence, 50019, Italy

ARTICLE INFO

Article history:
Received 14 February 2021
Received in revised form
1 March 2021
Accepted 1 March 2021
Available online 16 March 2021

Keywords:
Carbonic anhydrase
Enzyme inhibitors
Diazo compounds
The 'SAFE' protocol
Metal carbenes
N—H insertion
Primary sulfonamides
Stopped-flow assay
Nanomolar inhibition
Cancer cells
MTT-Test
Hypoxic environment

ABSTRACT

Herein we report the synthesis of a set of thirty-four primary sulfonamides generated *via* formal *N*—*H*-insertion of metal carbenes into anilinic amino group of sulfanilamide and its *meta*-substituted analog. Obtained compounds were tested *in vitro* as inhibitors of four physiologically significant isoforms of the metalloenzyme human carbonic anhydrase (*h*CA, EC 4.2.1.1). Many of the synthesized sulfonamides displayed low nanomolar K_i values against therapeutically relevant *h*CA II, IX, and XII, whereas they did not potently inhibit *h*CA I. Provided the promising activity profiles of the substances towards tumor-associated *h*CA IX and XII isozymes, single-concentration MTT test was performed for the entire set. Disappointingly, most of the discovered *h*CA inhibitors did not significantly suppress the growth of cancer cells either in normoxia or $CoCl_2$ induced hypoxic conditions. The only two compounds exerting profound antiproliferative effect turned out to be modest *h*CA inhibitors. Their out of the range activity in cells is likely attributive to the presence of Michael acceptor substructure which can potentially act either through the inhibition of Thioredoxin reductases (TrxRs, EC 1.8.1.9) or nonspecific covalent binding to cell proteins.

1. Introduction

Carbonic anhydrases (CA, EC 4.2.1.1) is a well-explored superfamily of methalloenzymes that catalyze the interconversion between carbon dioxide and bicarbonate ion ($CO_2 + H_2O \rightleftharpoons HCO_3^- + H^+$) in living organisms [1,2]. Eight evolutionary unrelated gene families have been identified so far, including α-, β-, γ-, δ-, ζ-, η-, θ, and ι-CAs [3—7]. In human, CAs are represented by 15 isoforms which differ significantly in terms of tissue distribution, catalytic activity and subcellular localization [8,9]. Thus, cytosolic (I, II, III, III, VII, XIII), mitochondrial (VA, VB) secreted (VI), and membrane-associated (IV, IX, XII, XIV) human (*h*) CA isozymes have been described [10,11]. Some *h*CAs play pivotal roles in fundamental physiological processes, such as CO_2-homeostasis, pH-regulation, electrolyte secretion, gluconeogenesis, lipogenesis, bone resorption, *etc.* [12,13]. Furthermore, their abnormal activity or expression profiles have been linked to a range of diseases, such as glaucoma, edema, obesity, neuropathic pain and cancer [14—20]. Accordingly, many *h*CA isoforms have been validated as valuable therapeutic targets and novel links to pathological disorders continue to be discovered [21—23].

Primary sulfonamides are the most investigated class of *h*CA inhibitors [24]. Indeed, many aromatic sulfonamides exert

* Corresponding author.
** Corresponding author.
E-mail addresses: claudiu.supuran@unifi.it (C.T. Supuran), m.krasavin@spbu.ru (M. Krasavin).

https://doi.org/10.1016/j.ejmech.2021.113352
0223-5234/

profound pan-isoform inhibitory activity against *h*CAs (Fig. 1A) [25]. In the meantime, the design of therapeutically relevant isozyme-selective agents traditionally relies on the 'tail-approach' [26]. This strategy implies decoration of the aromatic sulfonamide warhead with various 'tails' capable of interacting with non-conservative amino acid residues on the middle and outer parts of the active site cavity, thus conferring improved ligand binding and isozyme selectivity [27–31]. It is this approach which gave rise to a range of highly potent and selective inhibitors reported in last decades which are currently under extensive evaluation in pre-clinical or clinical settings (Fig. 1B) [32–35].

Despite the fact, that numerous X-ray structures of *h*CAs with small molecule ligands are available nowadays, rational approaches to the structure-based design of isozyme-selective inhibitors are still in their infancy [38–40]. Therefore, screening of small molecule compound libraries (preferably meeting the 'tail-approach' requirements) remains the main source of the insights on the structure-activity relationship (SAR) of inhibitors targeting various therapeutically relevant *h*CA isoforms [41]. Thus, extensive synthetic efforts furnishing versatile drug-like sulfonamides are of importance in medicinal chemistry as they serve to further decipher the design principles of the isozyme selective *h*CA inhibitors as well as investigate the translation of their inhibitory properties into the desired response in cell culture/animal disease models and in human [42].

Diazo compounds are valuable building blocks furnishing metal carbenoid intermediates for the synthesis of vast variety of medicinally relevant scaffolds [43]. However, the generation of diazo compounds has been traditionally associated with sulfonyl azide-based diazo transfer reagents known to be unsafe in handling due to the high potential of explosion hazards [44]. This limitation often motivated researchers to look for alternative synthetic routes (which is especially true in the context of industrial applications) and hampered the exploration of chemical space areas accessible *via* diazo chemistry [44]. To address the said inconveniences, we recently reported the sulfonylazide-free ('SAFE') protocol for the generation of diazo compounds in basic aqueous medium (Scheme 1) [45].

Furthermore, we have demonstrated that using this protocol, diazo compounds generated *in situ* can be further employed for parallel and diversity-oriented synthesis of small molecules which is of utmost importance for medicinal chemistry [45]. Indeed, such approach allowed us to cover hitherto unexplored chemical space by involving diazo compounds in diverse reactions yielding novel derivatives of various privileged scaffolds (Fig. 2) [46–50].

Among other findings, we showed that $Rh_2(esp)_2$-catalyzed coupling of α-diazo-γ-butyrolactams with aromatic amines can be performed with moderate to good yields [51]. Remarkably the reaction displayed tolerance to the presence of such functional groups as primary sulfonamide (Scheme 2) [51]. This gave us an idea that diazo compounds can be employed in the generation of small molecule sulfonamide libraries within our research program aiming at development of *h*CA inhibitors.

Herein we report the results of our study including preparation of novel sulfonamide-bearing small molecules from mono- and dicarbonyl diazo compounds as well as evaluation of their *h*CA inhibitory and antiproliferative profile.

2. Results and discussion

2.1. Synthesis of a set of primary sulfonamides

The coupling of α-diazo-γ-butyrolactams **14a-c** with 4-aminobenzenesulfonamide **12a** was performed as reported earlier [51]. Briefly, α-diazo-γ-butyrolactams **14a-c** were dissolved in anhydrous 1,4-dioxane and **12a** was added along with $Rh_2(esp)_2$ catalyst (1 mol%). The reaction was complete within 10 min at room temperature and furnished corresponding sulfonamide-bearing lactams **15a-c** in modest to good yields (Scheme 3).

While α-diazo-γ-butyrolactams reacted with **12a** at ambient conditions (their high reactivity apparently stems from the certain ring strain and decreased conjugation of the carbene anion with the carbonyl group), linear α-diazo monocarbonyl compounds **16** were less reactive and hence somewhat more forcing reaction conditions were required. After brief experimentation, we modified the reaction protocol using the mixture of 1,4-dioxane and toluene (3:4) which ensured both reasonable heating and dissolution of the reagents. This allowed for the preparation of compounds **17a-l** using sulfonamides **12a** (R^3 = 4-SO_2NH_2) and **12b** (R^3 = 3-SO_2NH_2) in modest to moderate yields (Scheme 4).

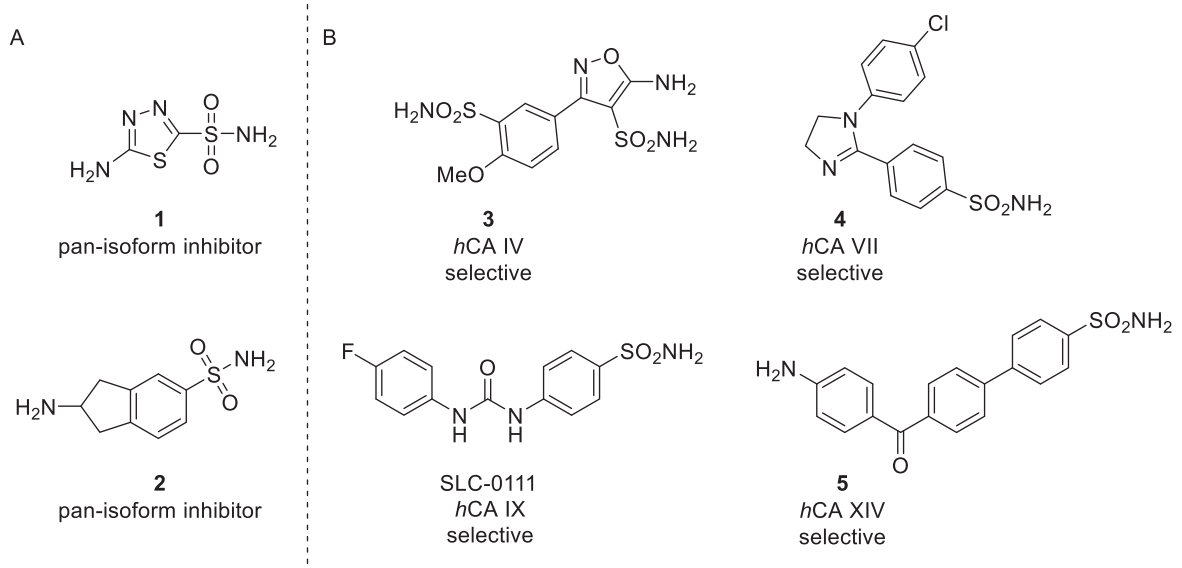

Fig. 1. (A) Examples of aromatic sulfonamide-based pan-isoform hCA inhibitors **1** [36] and **2** [37]. (B) Examples of potent and isozyme selective *h*CA inhibitors **3** [32], **4** [33], **5** [34] and SLC-0111 [35] designed using the 'tail-approach'.

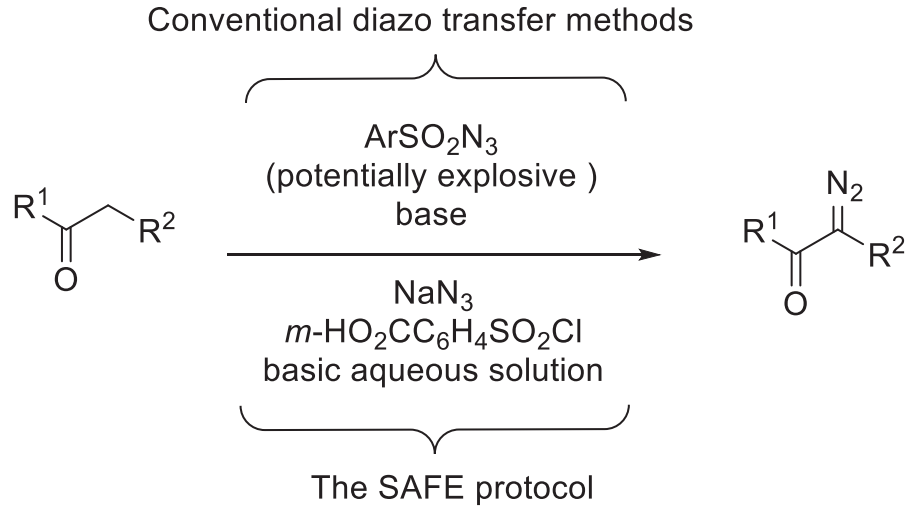

Scheme 1. 'SAFE' approach for the *in situ* generation of diazo compounds [45].

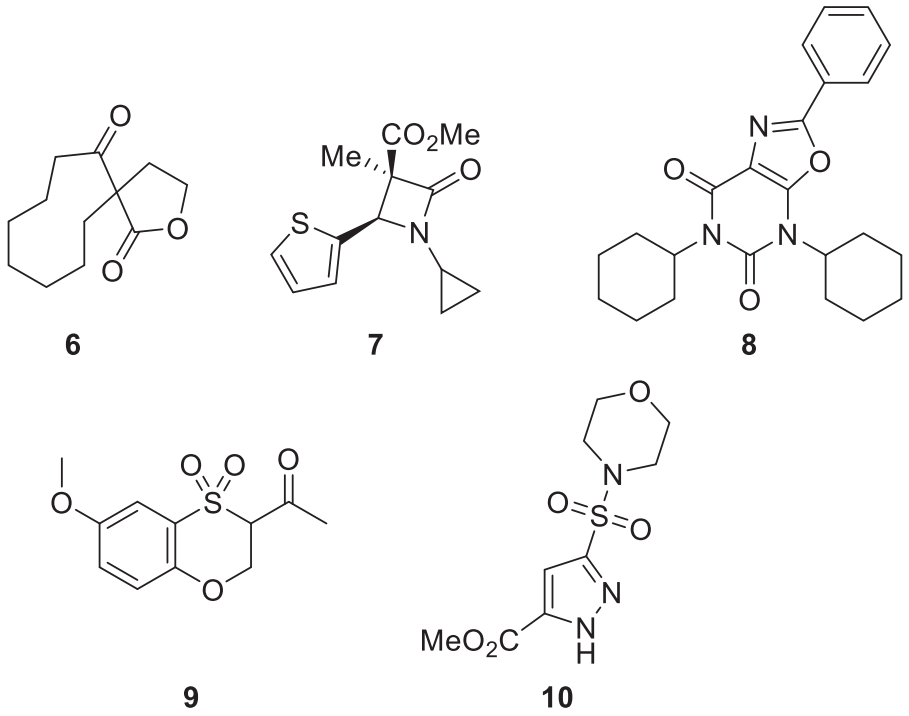

Fig. 2. Examples of privileged scaffold-based small molecules **6** [46], **7** [47], **8** [48], **9** [49], and **10** [50] synthesized in our group with the use of diazo compounds obtainable *via* the 'SAFE' protocol.

Noticeably, when linear 1,3-dicarbonyl diazo compounds **18** were introduced to the reaction with **12a**,**b** in some cases the Wolf rearrangement [34] was observed under the same conditions. Individual compounds were then isolated using column chromatography. Thus, not only *N*–*H* insertion products **19a-j** were obtained in modest to good yields, but also Wolf rearrangement products **20a-f** as shown in Scheme 5. It should be noted that for compounds **19f** and **20e** the ^{1}H NMR spectra display two partially overlapping sets of signals due to keto-enol tautomerism (see Experimental Section).

Finally, (*E*)-3-arylidene-4-diazopyrrolidine-2,5-diones **21a-c** were employed in the same reaction. Interestingly, in addition to the *N*–*H* insertion, double bond migration was observed under the reaction conditions, furnishing maleimides **22a-c** in good yields (Scheme 6).

2.2. Inhibitory profiles of the synthesized compounds against a panel of hCAs

We investigated the *h*CA inhibitory activities of the synthesized compounds by means of the stopped-flow carbon dioxide hydratase assay in comparison to acetazolamide (AAZ) as reference CAI [52]. The panel of enzymes included four physiologically significant isoforms, the cytosolic *h*CA I and II, as well as the transmembrane,

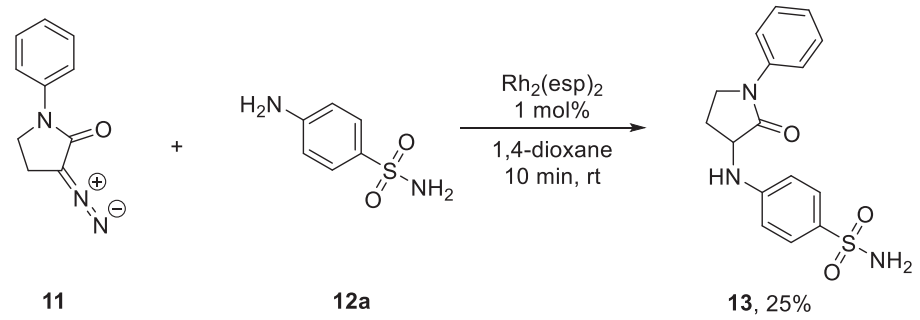

Scheme 2. $Rh_2(esp)_2$-catalyzed coupling of α-diazo-γ-butyrolactam **11** with 4-aminobenzenesulfonamide **12a** [51].

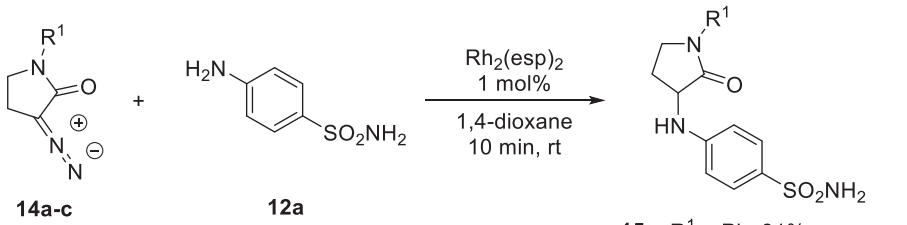

Scheme 3. Synthesis of sulfonamide-bearing γ-butyrolactam derivatives **15a-c**.

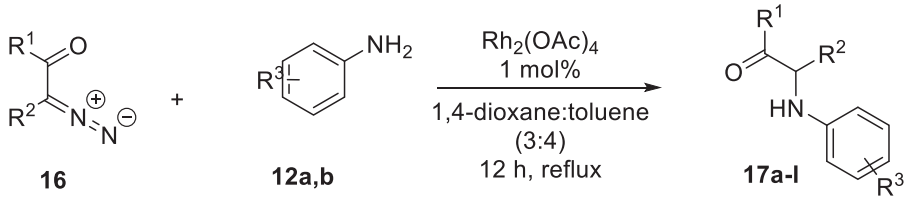

17a: R^1 = 4-MeC_6H_4, R^2 = H, R^3 = 4-SO_2NH_2 (25%)
17b: R^1 = 4-MeC_6H_4, R^2 = H, R^3 = 3-SO_2NH_2 (68%)
17c: R^1 = 4-$MeOC_6H_4$, R^2 = H, R^3 = 4-SO_2NH_2 (44%)
17d: R^1 = 4-$MeOC_6H_4$, R^2 = H, R^3 = 3-SO_2NH_2 (41%)
17e: R^1 = *t*-Bu, R^2 = H, R^3 = 3-SO_2NH_2 (23%)
17f: R^1 = Et_2N, R^2 = H, R^3 = 4-SO_2NH_2 (18%)
17g: R^1 = Et_2N, R^2 = H, R^3 = 3-SO_2NH_2 (24%)
17h: R^1 = OEt, R^2 = 4-ClC_6H_4, R^3 = 4-SO_2NH_2 (7%)
17i: R^1 = OEt, R^2 = 3,4-$(MeO)_2C_6H_3$, R^3 = 4-SO_2NH_2 (22%)
17j: R^1 = 4-$ClC_6H_4CH_2$-piperazine, R^2 = H, R^3 = 4-SO_2NH_2 (25%)
17k: R^1 = 4-$ClC_6H_4CH_2$-piperazine, R^2 = H, R^3 = 3-SO_2NH_2 (29%)
17l: R^1, R^2 = -$(CH_2)_5$-, R^3 = 4-SO_2NH_2 (41%)

Scheme 4. Coupling of linear α-diazo monocarbonyl compounds **16** with sulfonamides **12a,b**.

tumor-associated *h*CA IX and XII. The inhibitory profile of small molecules against those isozymes is of interest for drug discovery in a number of therapeutic areas [8,53,54]. For instance, *h*CA II and XII are upregulated in the eyes of patients suffering from glaucoma and are validated targets for intraocular pressure-lowering agents [19]. In contrast, *h*CA IX (and *h*CA XII) proved valuable extracellular tumor biomarkers and their inhibitors attract growing attention for the needs of cancers treatment and prognosis [14,55,56]. Finally, cytosolic *h*CA I is considered an off-target enzyme for both anti-glaucoma and anticancer therapeutic applications of CAIs [57]. The results of the assay are outlined in Table 1.

The following structure-activity relationship trends can be unveiled from the inhibition data represented in Table 1.

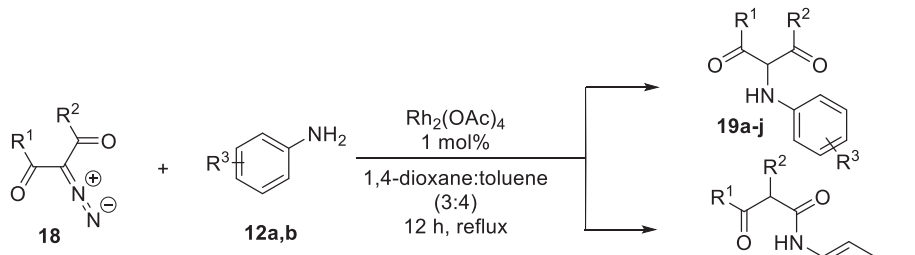

19a: $R^1 = R^2 = OMe$, $R^3 = 4\text{-}SO_2NH_2$ (35%)
19b: $R^1 = R^2 = OEt$, $R^3 = 4\text{-}SO_2NH_2$ (33%)
19c: $R^1 = R^2 = O\text{-}i\text{-}Pr$, $R^3 = 4\text{-}SO_2NH_2$ (18%)
19d: $R^1 = R^2 = O(CH_2)_2OMe$, $R^3 = 4\text{-}SO_2NH_2$ (70%)
19e: $R^1 = OMe$, $R^2 = CH_2OMe$, $R^3 = 4\text{-}SO_2NH_2$ (12%)
19f: $R^1 = OEt$, $R^2 = Ph$, $R^3 = 4\text{-}SO_2NH_2$ (66%)
19g: $R^1 = OEt$, $R^2 = Ph$, $R^3 = 3\text{-}SO_2NH_2$ (23%)
19h: $R^1 = OEt$, $R^2 = 4\text{-}MeOC_6H_4$, $R^3 = 4\text{-}SO_2NH_2$ (19%)
19i: $R^1 = OEt$, $R^2 = 4\text{-}MeOC_6H_4$, $R^3 = 3\text{-}SO_2NH_2$ (28%)
19j: $R^1 = OMe$, $R^2 = 2\text{-}MeOC_6H_4$, $R^3 = 4\text{-}SO_2NH_2$ (31%)
20a: $R^1 = OEt$, $R^2 = i\text{-}Pr$, $R^3 = 4\text{-}SO_2NH_2$ (38%)
20b: $R^1 = OEt$, $R^2 = i\text{-}Pr$, $R^3 = 3\text{-}SO_2NH_2$ (38%)
20c: $R^1 = OEt$, $R^2 = Ph$, $R^3 = 4\text{-}SO_2NH_2$ (28%)
20d: $R^1 = Ph$, $R^2 = i\text{-}Pr$, $R^3 = 4\text{-}SO_2NH_2$ (32%)
20e: $R^1 = Ph$, $R^2 = i\text{-}Pr$, $R^3 = 3\text{-}SO_2NH_2$ (41%)
20f: $R^1 = 4\text{-}ClC_6H_4$, $R^2 = Me$, $R^3 = 4\text{-}SO_2NH_2$ (41%)

Scheme 5. Reaction of linear 2-diazo 1,3-dicarbonyl compounds with sulfonamides **12a,b** leading to N–H insertion products **19a-j** or Wolf rearrangement products **20a-f**.

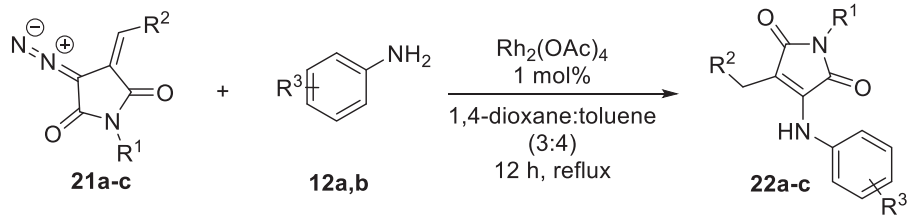

22a: $R^1 = 4\text{-}MeC_6H_4$, $R^2 = 4\text{-}ClC_6H_4CH_2$, $R^3 = 4\text{-}SO_2NH_2$ (71%)
22b: $R^1 = 4\text{-}MeC_6H_4$, $R^2 = 4\text{-}ClC_6H_4CH_2$, $R^3 = 3\text{-}SO_2NH_2$ (69%)
22c: $R^1 = Ph$, $R^2 = 2\text{-}MeOC_6H_4CH_2$, $R^3 = 4\text{-}SO_2NH_2$ (51%)

Scheme 6. Reaction of (E)-3-Arylidene-4-diazopyrrolidine-2,5-diones with sulfonamides **12a,b**.

(i) Many of the generated compounds tend to possess moderate or weak inhibitory activity against the cytosolic isoform *h*CA I. Indeed, inhibition constants (K_i's) for sulfonamides **17i**, **17k**, **19i**, and **20e** ranged between 1357 and 5876 nM, whereas for **22a-c** they exceeded 10 000 nM. Most of the remaining representatives blocked the enzyme's activity at sub-micromolar concentrations, similarly to the standard AAZ (Ki 250 nM). However, **15a**, **17a**, **17g**, **19d**, **19e**, and **20a** displayed double-digit nanomolar (i.e. 53.3–85.8 nM) K_i values thus outperforming the reference drug. Noticeably, within the homologous range of compounds **19a-c** the inhibitory activity against *h*CA I increased with the growth of lipophilicity with K_i's 166.5 nM (R^1, R^3 = OMe), 134.9 nM (R^1, R^2 = OEt), and 105.3 nM (R^1, R^2 = O-*i*-Pr) respectively. Furthermore, compound **19d** (R^1, R^2 = $O(CH_2)_2OMe$) showed even better inhibition of this isozyme with K_i of 85.8 nM. Interestingly, among dicarbonyl derivatives **19a-j**, **20a-f** *p*-aminobenzenesulfonamide bearing compounds were nearly one order of magnitude more potent *h*CA I inhibitors as compared to the *m*-substituted counterparts. This can be exemplified with cases like the following: **19f** (R^3 = 4-$H_2NSO_2C_6H_4$, K_i 245.4 nM) *vs* **19g** (R^3 = 3-$H_2NSO_2C_6H_4$, K_i 1566 nM); **20d** (R^3 = 4-$H_2NSO_2C_6H_4$, Ki 182.8 nM) *vs* **20e** (R^3 = 3-$H_2NSO_2C_6H_4$, Ki 1357 nM) and so on. Meanwhile, this tendency was not observed among monocarbonyl derivatives **17a-l.** Among all tested compounds **17a** turned out to show the highest activity against *h*CA I with the K_i value of 53.3 nM.

(ii) Inhibitory activity of the tested substances against the physiologically dominant *h*CA II isoform was generally higher than that versus *h*CA I. In fact, the K_i's of the vast majority of the compounds laid in the double-digit nanomolar region. Encouragingly, three derivatives **15b**, **19j**, and **20d** turned out to be low nanomolar inhibitors of *h*CA II displaying K_i's 8.1, 5.9, and 6.2 nM correspondingly. Together with **19f** (K_i 11.3 nM) these frontrunners outperformed the

Table 1
Inhibition data of human *h*CA isoforms hCA I, II, IX and XII for compounds **15a-c**, **17a-l**, **19a-j**, **20a-f** and **22a-c** using acetazolamide (AAZ) as a reference.

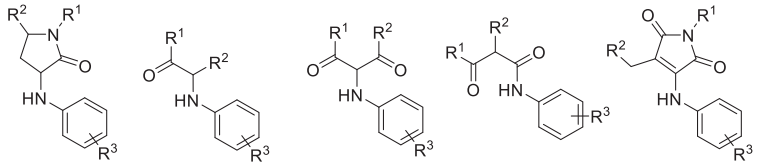

Cmpd	R^1	R^2	R^3	K_i (nM)[a]			
				*h*CA I	*h*CA II	*h*CA IX	*h*CA XII
15a	Ph	H	4-SO_2NH_2	62.0	36.9	9.5	24.9
15b	3-$CF_3C_6H_4$	H	4-SO_2NH_2	462.9	8.1	19.7	13.8
15c	2-thiazolyl	H	4-SO_2NH_2	137.6	25.8	36.8	18.8
17a	4-MeC_6H_4	H	4-SO_2NH_2	53.3	43.4	15.2	67.4
17b	4-MeC_6H_4	H	3-SO_2NH_2	293.8	94.9	63.9	208.4
17c	4-$MeOC_6H_4$	H	4-SO_2NH_2	124.5	38.6	10.1	81.7
17d	4-$MeOC_6H_4$	H	3-SO_2NH_2	919.7	123.9	54.3	189.5
17e	*t*-Bu	H	3-SO_2NH_2	343.4	81.5	41.7	24.1
17f	Et_2N	H	4-SO_2NH_2	242.7	144.1	89.1	33.2
17g	Et_2N	H	3-SO_2NH_2	70.6	123.3	45.9	83.7
17h	OEt	4-ClC_6H_4	4-SO_2NH_2	134.8	154.7	54.3	63.0
17i	OEt	3,4-$(MeO)_2C_6H_3$	4-SO_2NH_2	5876	73.5	6.5	35.7
17j	4-$ClC_6H_4CH_2$-piperazine	H	4-SO_2NH_2	146.4	78.1	21.2	11.3
17k	4-$ClC_6H_4CH_2$- piperazine	H	3-SO_2NH_2	3951	409.6	116.1	36.1
17l	4-$ClC_6H_4CH_2$- piperazine	H	4-SO_2NH_2	202.3	91.6	6.4	49.2
19a	OMe	OMe	4-SO_2NH_2	166.5	71.8	58.1	72.4
19b	OEt	OEt	4-SO_2NH_2	134.9	27.6	52.4	57.2
19c	O-*i*-Pr	O-*i*-Pr	4-SO_2NH_2	105.3	20.3	28.1	61.4
19d	$O(CH_2)_2OMe$	$O(CH_2)_2OMe$	4-SO_2NH_2	85.8	18.5	36.8	45.0
19e	OMe	CH_2OMe	4-SO_2NH_2	69.8	55.2	64.1	24.7
19f	OEt	Ph	4-SO_2NH_2	245.4	11.3	18.0	21.8
19g	OEt	Ph	3-SO_2NH_2	1566	277.6	58.6	82.9
19h	OEt	4-$MeOC_6H_4$	4-SO_2NH_2	313.9	28.6	12.5	16.5
19i	OEt	4-$MeOC_6H_4$	3-SO_2NH_2	2547	161.3	91.9	167.6
19j	OMe	2-$MeOC_6H_4$	4-SO_2NH_2	828.8	5.9	25.6	26.5
20a	OEt	*i*-Pr	4-SO_2NH_2	56.9	66.3	32.0	66.2
20b	OEt	*i*-Pr	3-SO_2NH_2	345.8	87.5	70.1	113.5
20c	OEt	Ph	4-SO_2NH_2	310.5	57.2	61.5	41.6
20d	Ph	*i*-Pr	4-SO_2NH_2	182.8	6.2	30.1	35.6
20e	Ph	*i*-Pr	3-SO_2NH_2	1357	98.7	71.1	59.6
20f	4-ClC_6H_4	Me	4-SO_2NH_2	215.2	48.0	34.3	22.6
22a	4-MeC_6H_4	4-ClC_6H_4	4-SO_2NH_2	>10 000	2751	81.9	128.5
22b	4-MeC_6H_4	4-ClC_6H_4	3-SO_2NH_2	>10 000	3163	635.2	1067
22c	Ph	2-$MeOC_6H_4$	4-SO_2NH_2	>10 000	4635	68.0	87.9
AAZ	-			250	12.5	25.0	5.7

**R^1, R^2 = $-(CH_2)_5-$.
[a] Mean from three different assays, by a stopped flow technique (errors were in the range of ± 5−10% of the reported values).

reference drug AAZ whose K_i value was 12.5 nM. In contrast, maleimides **22a-c** again showed negligible inhibition of the enzyme, as their Ki's ranged between 2751 and 4635 nM. As in the case of *h*CA I, the inhibition activity against *h*CA II increased in the range of compounds **19a-d** with K_i's 71.8 nM (R^1, R^3 = OMe), 27.6 nM (R^1, R^2 = OEt), 20.3 nM (R^1, R^2 = O-*i*-Pr), and 18.5 nM (R^1, R^2 = $O(CH_2)_2OMe$) respectively. It should be also noted that similarly to *h*CA I, *h*CA II isoform was sensitive to the substitution pattern of the dicarbonyl derivatives **19a-j**, **20a-f** with clear one order of magnitude drop of the Ki values for the *m*-aminobenzenesulfonamide bearing analogs. Thus, *meta*-position of the sulfonamide function within the benzenesulfonamide warhead can be considered generally detrimental pattern for the compounds' inhibitory activity against cytosolic *h*CA I and II isoforms.

(iii) As opposed to the cytosolic isozymes, tumor-associated transmembrane protein *h*CA IX was nearly insensitive to the differences between *m*- and *p*-aminobenzenesulfonamide bearing derivatives. Indeed, most of the reported compounds showed very efficient inhibitory activity also against these isozymes with double-digit nanomolar K_i values prevailing throughout the whole set. These values were comparable to the reference drug AAZ (K_i 25.0 nM). Therefore, it can be concluded that the synthesized molecules are flexible enough to efficiently adopt the catalytic cavity of *h*CA IX and no substantial hindrance is conferred with the introduced substituents. Meanwhile, several most potent inhibitors can be highlighted, such as **15a**, **17c**, **17i**, **17l**, and **19h** exhibiting Ki's in the range between 6.4 and 12.5 nM. Interestingly, three of them (**17c**, **17i**, **19h**) incorporated alkoxy-substituted aromatic moieties as the 'tail' motif. In contrast, the only compound exhibiting less pronounced, submicromolar activity toward *h*CA IX isoform turned out to be **22b,** a maleimide derivative endowed with the *m*-aminobenzenesulfonamide warhead.

(iv) Turning to another transmembrane isozyme – *h*CA XII, known as promising target in the context of glaucoma management as well as therapy of solid tumors, again, remarkable activity of many of generated compounds could be observed. Specifically, **15b**, **17j**, and **19h** exhibited K_i's between 11.3 and 16.5, therefore approaching the efficiency level of AAZ (K_i 5.7 nM). Three compounds with K_i values above 100 nM, (**17d**, **19i**, **22b**) incorporated *m*-aminobenzenesulfonamide warhead which is apparently undesirable in the context of *h*CA XII inhibition as well.

(v) Taking a closer look at the compounds' isoform-selectivity profiles the following trends can be highlighted. Most of compounds were less potent against *h*CA I compared to the other *h*CA isoforms which is considered beneficial for the medicinal applications of CAIs. It can be seen from Table 1 that the *m*-aminobenzenesulfonamide bearing compounds were generally less active against all isoforms in question in comparison to the *p*-aminobenzenesulfonamide-substituted counterparts. However, the activity drop for the *meta*-substituted derivatives was somewhat uneven. Indeed, such substitution pattern tended to confer higher selectivity toward transmembrane *h*CA IX and XII over cytosolic enzymes. Compounds **19f** and **19g** can serve as examples for this trend. Thus, upon the shift from the *p*-to the *m*-substituted warheads a 6.4-fold (from 245.4 to 1566 nM) activity decrease was observed against *h*CA I, and 24.6-fold (from 11.3 to 277.6) against hCA II. On the other hand, for the transmembrane *h*CAIX and *h*CA XII isozymes only 3.3 (from 18.0 to 58.6 nM) and 3.8 (form 21.8–82.9 nM) fold activity drop was observed, respectively, thus showing that **19g** is selective to *h*CAIX and *h*CA XII. Aryl-substituted monocarbonyl derivatives **17c, 17d, 17i** and **17l** displayed certain level of selectivity towards *h*CA IX. Of these substances, compound **17l** incorporating cycloheptan-2-one fragment was the most potent and displayed the most attractive profile with the K_i ratios of 31.6 (*h*CA I/*h*CA IX) and 14.3 (*h*CA II/*h*CA IX). Interestingly, *m*-aminobenzenesulfonamide-bearing compound **17k** acted as potent and selective *h*CA XII inhibitor, while *para*-substituted **17j** also strongly affected *h*CA IX. Diazocarbonyl compound **19g** decorated with *m*-aminobenzenesulfonamide proved selective towards *h*CA IX/XII over the cytosolic isozymes. In contrast, **19j** demonstrated selectivity toward *h*CA II. The latter profile was very close to that of **20d,** whereas Wolf rearrangement products **20a-c**, **20e** and **20f** were generally double-digit nanomolar inhibitors of *h*CA II, IX and XII and displayed certain variations in their affinity to the off-target *h*CA I. Finally, it should be noted that despite their modest inhibitory activities, *p*-aminobenzenesulfonamide substituted maleimide derivatives **22a** and **22c** showed remarkable selectivity towards tumor associated isoforms. For instance, the K_i ratios of **22c** were found to be 147.1 (*h*CA I/*h*CA IX) and 68.2 (*h*CA II/*h*CA IX). Summing up, many of generated compounds displayed attractive selectivity profiles, in contrast to the reference inhibitor AAZ. In particular, the low-nanomolar activity of compounds **15b, 19j**, and **20d** against glaucoma-related *h*CA II and *h*CA XII, in combination with their high selectivity over the off-target *h*CA I render them promising in the context of continuing search for intraocular-pressure lowering agents with enhanced safety level and duration of action [16,58]. On the other hand, several potent and selective inhibitors of *h*CA IX/XII such as **17i**, **17l**, and **19h**, demonstrated attractive profiles for the anticancer drug development as these isoforms play crucial roles in a range of cancer-related pathological processes [50].

2.3. Antiproliferative activity against cancer and normal cell lines

Among the potential clinical applications of *h*CA inhibitors, tumor diagnostic and treatment has drawn the most significant attention in the last decade [59]. Indeed, numerous studies showed that overexpression of *h*CA IX and XII isoforms can serve as a robust marker of malignant tissues [60,61]. Therefore, a wide range of fluorescent and radiolabeled agents for tumor-visualization have been developed, basing on either *h*CA IX/XII targeting biomolecules or sulfonamide-bearing small molecular ligands [55,62]. Furthermore, the catalytic activity of *h*CA IX and XII largely ensures the adaptation of tumor cells to unfavorable growth conditions characterized by hypoxia and lack of nutrients [63]. In particular, the catalytic activity of the extracellular domain of these enzymes plays a key role in the functioning of a number of transport proteins and helps avoid intracellular acidosis (maintaining the slightly alkaline intracellular pH) [64,65]. At the same time, the extracellular acidification induced by *h*CA IX (on average the microenvironment of hypoxic tumors is characterized by pH 6.5–6.8) [66] can contribute to the disruption of intercellular adhesion contacts by suppressing the adhesion protein E-cadherin, as well as transformation of malignant cells into a less differentiated state [67] In this case, cancer cells acquire the so-called "stem-like" phenotype (an increase in the proportion of cancer stem cells in the tumor), which makes the tumor phenotype more aggressive and resistant to many chemotherapeutic drugs [60]. Thus, recent data indicate the multiple roles that *h*CA IX and XII isoforms play in the survival and proliferation of cancer cells.

It should be stressed, however, that the discovery of anticancer agents based on the small molecule *h*CA inhibitors is not a straightforward task. Despite the fact that several clinical studies are in progress employing well-known *h*CA inhibitors AAZ [68,69] or SLC-0111 [35] as antineoplastic agents in combined therapy of aggressive tumors, certain aspects remain unraveled in the process of identification of novel promising drug candidates. Our recent literature data analysis highlighted that potent inhibitory activities of sulfonamides against isolated recombinant *h*CA IX and XII is often not translated into antiproliferative properties at the stage of 2D cell culture models [42]. Considering that multiple reasons can be assumed in each particular case (e. g., insufficient metabolic stability of the molecule, it's binding to off-target proteins etc.), further screening efforts and biochemical studies are highly desired in order to shed more light on this problem.

Provided our compounds revealed remarkable potency against tumor-associated *h*CA IX and *h*CA XII we became interested in evaluating their antiproliferative activity. To this end, we performed the well-established MTT test in 96-well plate format. Since, the expression of *h*CA IX in tumor cells is controlled by hypoxia-inducible factor 1α (HIF-1α) [50] we employed both normoxic conditions and $CoCl_2$-induced hypoxia to perform the study [70]. The results of a single-concentration screening against human breast cancer cell lines MDA-MB-231 and MCF-7 are presented in Figs. 3 and 4, respectively.

As evident from the screening results, compounds **15a-c**, **17a-l**, **19a-i**, and **20a-e** exhibited either no or mild antiproliferative activity against both cancer cell lines at 100 μM concentration. Of note, no significant difference was observed between the compounds' profiles under normoxic and hypoxic conditions. Discouragingly, many of the discovered highly potent *h*CA IX/XII inhibitors did not exert noticeable antiproliferative activity. From the entire subset only four compounds **17h** (K_i (*h*CA IX) 54.3 nM; K_i (*h*CA XII) 63.0 nM), **17l** (K_i (*h*CA IX) 6.4 nM; K_i (*h*CA XII) 49.2 nM), **19g** (K_i (*h*CA IX) 58.6 nM; K_i (*h*CA XII) 82.9 nM), and **20f** (K_i (*h*CA IX) 34.3 nM; K_i (*h*CA XII) 22.6 nM) induced at least 30% decrease of the MDA-MB-231 cell line viability. Furthermore, MCF-7 was only sensitive to **17c**

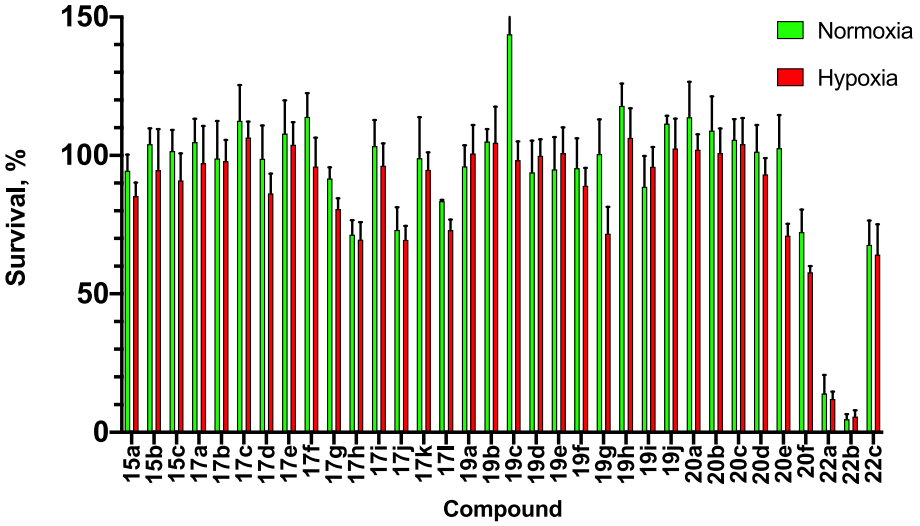

Fig. 3. Cell viability MTT assay results for compounds **15a-c**, **17a-l**, **19a-i**, **20a-e** and **22a-c** at 100 μM concentration against MDA-MB-231 cell line under normoxic (shown in green) and hypoxic conditions (100 μM $CoCl_2$, shown in red). Values are displayed in % as the mean ± SEM of three experiments relative to control (0 μM, 100% viability, not shown).

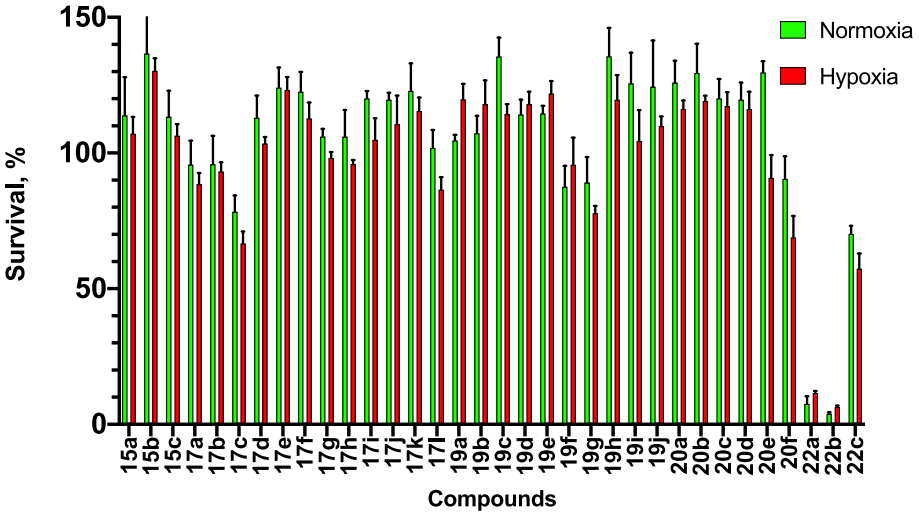

Fig. 4. Cell viability MTT assay results for compounds **15a-c**, **17a-l**, **19a-i**, **20a-e** and **22a-c** at 100 μM concentration against MCF-7 cell line under normoxic (shown in green) and hypoxic conditions (100 μM $CoCl_2$, shown in red). Values are displayed in % as the mean ± SEM of three experiments relative to control (0 μM, 100% viability, not shown).

(K_i (*h*CA IX) 10.1 nM; K_i (*h*CA XII) 81.7 nM) and **20f**. On the other hand, maleimide derivatives **22a-c** revealed profound antiproliferative action. Moreover, it was not the relatively potent *h*CA inhibitor **22c** showing better anticancer properties. Instead, **22a** and especially **22b** with micromolar to submicromolar *h*CA Ki values decreased cancer cells viability to the level of 10% and below.

Altogether, the obtained results confirmed the observation that low K_i values against recombinant *h*CA IX/XII cannot be considered as robust predictive factor regarding the anticancer potential of sulfonamides. Indeed, neither of the low nanomolar *h*CA IX/XII inhibitors identified in this study exerted substantial influence at cancer cells growth under normoxic or hypoxic conditions, with best results comprising only *ca.* 30% of cell viability reduction. In the meantime, treatment of cancer cells with less anti-*h*CA active derivatives **22a** and **22b** caused dramatic drop in the cancer cell survival. High Ki values against the enzymes in question suggest that the observed anticancer activity could unlikely be attributed to the inhibition of *h*CA IX/XII. It should be taken into account that these compounds incorporated another cytotoxicity-associated motif, i.e. mild Michael acceptor electrophile. On the one hand, Michael acceptors are known to block the activity of Thioredoxin reductases (TrxRs, EC 1.8.1.9) which are another class of anticancer drug targets attracting growing attention in recent years [69]. We have previously hypothesized that combination of CAI and TrxR inhibitory motifs within one chimeric compound can be a valuable strategy for the design of antiproliferative agents [69]. Furthermore, there is a range of examples present in literature where such combinations occasionally emerged, leading to increased cytotoxicity [71–74]. On the other hand, Michael acceptors has been known as so-called pan-assay interference compounds (PAINS) [75]. Despite the fact that the presence of this motif in the CAIs apparently does not lead to the false positive results within the stopped-flow CO_2 hydratase assay [71–74], cell-based screening results for such compounds should be taken with great caution [75]. With these considerations in mind we made additional efforts to validate our observations. In particular, IC_{50} values were determined for two most active compounds **22a** and **22b** against MDA-MB-231 and MCF-7 cells as well as against normal cell line WI-26 VA4 (Table 2).

IC_{50} values of both **22a** and **22b** laid within the range between 10.84 and 37.21 μM against all used cell lines either under normoxic or hypoxic conditions. In contrast to what can be seen expected from the single-concentration screening results, EC_{50} values of **22a** were slightly lower than those of **22b**. In the meantime, no significant gap between the sensitivity of malignant or healthy cell cultures towards the tested agents was observed. Thus, despite the fact that antiproliferative action of **22a** and **22b** turned out to be dose-dependent (see Supporting information for the dose-response curves), these compounds did not show any selectivity towards malignant cells over healthy once and therefore their potential for medicinal application remains unclear.

3. Conclusion

We demonstrated that diazo compounds can be efficiently used for the generation of structurally diverse small molecule sulfonamides which are highly desired in the context of *h*CA inhibition-related research domain. Inhibitory profiles of 34 newly synthesized compounds against a panel of four physiologically significant *h*CA isoforms (*h*CA I, II, IX and XII) have been determined. Interestingly, the obtained molecules tended to possess selectivity toward the therapeutically relevant *h*CA or *h*CA IX/XII over *h*CA I which is considered an off-target protein. Furthermore, certain substances displayed low nanomolar K_i values against one or several of these isoforms. Considering the promising inhibitory activity of the generated molecules with respect to tumor-associated *h*CA IX and XII, their antiproliferative properties have been evaluated. Discouragingly, human breast cancer cell lines MDA-MB-231 and MCF-7 displayed only a modest decrease in cell viability when treated with 100 μM of the obtained low nanomolar *h*CA inhibitors. In contrast, a couple of least active *h*CA blockers exhibited profound antiproliferative properties, which is likely attributive of the mild Michael acceptor motif present in their structures. In the meantime, the potential of the synthesized compounds as intraocular pressure lowering agents remains to be evaluated and will be reported in due course.

4. Experimental section

4.1. General experimental procedures

Diazo compounds used in this study were prepared as previously reported [45,76,77] other reagents were obtained from commercial sources and used without additional purification. 1,4-Dioxane and toluene were distilled from suitable drying agents. Mass spectra were recorded with a Bruker Maxis HRMS-ESI-qTOF spectrometer (electrospray ionization mode). NMR spectroscopic data were recorded with Bruker Avance 400 spectrometer (400.13 MHz for ^{1}H, 100.61 MHz for ^{13}C and 376.50 MHz for ^{19}F) and were referenced to residual solvent proton peaks and solvent carbon peaks. HPLC preparative chromatography was performed with Agilent PrepHT XDB-C18 preparative cartridge 21.2 × 150 mm 5 μm. Product **15c** was purified by HPLC eluting with H_2O–MeCN with addition of 0.1% TFA (elution gradient MeCN: 40 → 60%); flow rate 12 mL/min, column temperature 40 °C.

Table 2
IC_{50} values determined for maleimides **22a** and **22b** against cancer cell lines MDA-MB-231 and MCF-7 and one normal cell line WI-26 VA4.

Compounds	IC_{50}, μM[a]					
	MCF7		MDA-MB-231		WI-26 VA4	
	Normoxia	Hypoxia	Normoxia	Hypoxia	Normoxia	Hypoxia
22a	10.84	11.52	16.55	15.61	21.91	26.15
22b	14.90	15.28	37.21	36.77	22.03	35.61

[a] Compound concentration required to reduce cell proliferation by 50%, as determined with the MTT method, under conditions allowing untreated controls to undergo at least two consecutive rounds of multiplication. Data represent mean values from three independent determinations.

4.1.1. General procedure (GP 1) for the preparation of sulfonamides *15a-c*

Aminobenzenesulfonamide **12a,b** (0.29 mmol) and corresponding diazo lactam **14** (0.29 mmol) were dissolved in dry 1,4-dioxane (5 mL). Rh_2esp_2 (1 mol-%) was added as catalyst and the emission of nitrogen was observed. The mixture was stirred for 10 min and concentrated *in vacuo*. Obtained residues were purified by column chromatography on silica gel using chloroform/MeOH as an eluent to afford compounds **15a-c**. Compound **15c** was purified by HPLC as described above.

*4.1.1.1. 4-((2-Oxo-1-phenylpyrrolidin-3-yl)amino)benzenesulfonamide (**15a**).* Yield 55 mg (31%). Beige solid, m.p. 228.1–229.5 °C. ^{1}H NMR (400 MHz, DMSO-d_6) δ 7.72 (d, J = 8.0 Hz, 2H, ArH), 7.54 (d, J = 8.7 Hz, 2H, ArH), 7.41 (t, J = 7.9 Hz, 2H, ArH), 7.17 (t, J = 7.4 Hz, 1H, ArH), 6.94 (s, 2H, NH_2), 6.79 (d, J = 8.8 Hz, 2H, ArH), 6.70 (d, J = 7.5 Hz, 1H, NH), 4.61–4.45 (m, 1H, CH- pyrrolid-2-one), 3.93–3.75 (m, 2H, CH_2- pyrrolid-2-one), 2.62 (dtd, J = 12.0, 8.2, 4.7 Hz, 1H, CH_2- pyrrolid-2-one), 1.94 (dq, J = 12.3, 9.4 Hz, 1H, CH_2-pyrrolid-2-one).^{13}C NMR (101 MHz, DMSO-d_6) δ 172.69, 151.31, 139.99, 131.27, 129.24, 127.69, 124.72, 119.75, 112.03, 55.00, 44.90, 26.52. HRMS (ESI) m/z $[M+Na]^+$ calculated for $C_{16}H_{17}N_3O_3SNa^+$ 354.0876, found 354.0883.

*4.1.1.2. 4-((2-Oxo-1-(3-(trifluoromethyl)phenyl)pyrrolidin-3-yl)amino)benzenesulfonamide (**15b**).* Yield 31 mg (61%). White amorphous solid. ^{1}H NMR (400 MHz, DMSO-d_6) δ 8.24 (s, 1H, ArH), 7.89 (d, J = 8.0 Hz, 1H, ArH), 7.67 (t, J = 8.1 Hz, 1H, ArH), 7.54 (dd, J = 7.9, 3.5 Hz, 3H, ArH), 6.95 (s, 2H, NH_2), 6.79 (d, J = 8.8 Hz, 2H, ArH), 6.72 (d, J = 7.7 Hz, 1H, NH), 4.64–4.53 (m, 1H, CH-pyrrolid-2-one), 3.98–3.83 (m, 2H, CH_2-pyrrolid-2-one), 2.70–2.58 (m, 1H, CH_2-pyrrolid-2-one), 2.05–1.90 (m, 1H, CH_2-pyrrolid-2-one). ^{13}C NMR (101 MHz, DMSO-d_6) δ ^{13}C NMR (101 MHz, DMSO) δ 172.94, 150.72, 140.10, 130.92, 130.07, 129.44 (d, J = 31.7 Hz), 127.20, 124.04 (q, J = 272.6 Hz), 122.57, 120.46 (q, J = 3.7 Hz), 115.47 (q, J = 4.2 Hz), 111.58, 54.47, 44.35, 25.76. HRMS (ESI) m/z $[M+Na]^+$ calculated for $C_{17}H_{16}F_3N_3O_3SNa^+$ 422.0755, found 422.0757.

*4.1.1.3. 4-((2-Oxo-1-(thiazol-2-yl)pyrrolidin-3-yl)amino)benzenesulfonamide (**15c**).* Yield 13 mg (15%). Beige solid, m.p. >300 °C. 1H NMR (400 MHz, DMSO-d_6) δ 7.59–7.50 (m, 3H, ArH, CH-thiazole), 7.35 (d, J = 3.5 Hz, 1H, NH), 6.95 (s, 2H, NH2), 6.78 (d, J = 8.8 Hz, 3H, ArH, CH-thiazole), 4.84–4.68 (m, 1H, CH-pyrrolid-2-one), 4.20 (ddd, J = 10.6, 9.1, 1.8 Hz, 1H, CH2- pyrrolid-2-one), 3.98–3.83 (m, 1H, CH2-pyrrolid-2-one), 2.66 (ddd, J = 14.0, 9.8, 7.4 Hz, 1H, CH2-pyrrolid-2-one), 2.15–1.96 (m, 1H, CH2-pyrrolid-2-one). 13C NMR (101 MHz, DMSO-d_6) δ 172.49, 157.54, 151.03, 138.18, 131.65, 127.74, 114.96, 112.14, 54.38, 44.94, 26.51. HRMS (ESI) m/z [M+H]+ calculated for C13H15N4O3S2+ 339.0579, found 339.0580.

4.1.2. General procedure (GP 2) for the preparation of sulfonamides *17a-l*, *19a-i*, *20a-e* and *22a-c*

Aminobenzenesulfonamide **12a,b** (0.29 mmol) was dissolved in 5 mL of dry mixture of 1,4-dioxane and toluene (3:4) under refluxing. Then corresponding diazo compound **16, 18, 21a-c** (0.35 mmol) and the catalyst $Rh_2(OAc)_4$ (1 mol-%) were added and the emission of nitrogen was observed. The mixture was refluxed overnight and concentrated *in vacuo*. Obtained residues were purified by column chromatography on silica gel using chloroform/

MeOH or DCM/EA as an eluent. Some of the resulting compounds (**19a**, **19c**, **22a-c**) precipitated and did not require additional purification.

*4.1.2.1. 4-((2-Oxo-2-(p-tolyl)ethyl)amino)benzenesulfonamide (**17a**).* Yield 89 mg (23%). Beige solid, m.p. 220.0–221.9 °C. 1H NMR (400 MHz, DMSO-d_6) δ 7.98 (d, J = 8.1 Hz, 2H, ArH), 7.53 (d, J = 8.9 Hz, 2H, ArH), 7.38 (d, J = 7.9 Hz, 2H, ArH), 6.93 (s, 2H, NH2), 6.75 (d, J = 8.9 Hz, 2H, ArH), 6.58 (t, J = 5.5 Hz, 1H, NH), 4.74 (d, J = 5.5 Hz, 2H, CH2), 2.41 (s, 3H, Me). 13C NMR (101 MHz, DMSO-d_6) δ 195.96, 151.45, 144.58, 132.99, 131.15, 129.81, 128.48, 127.66, 111.89, 49.78, 21.69. HRMS (ESI) m/z [M − H]+ calculated for C15H15N2O3S+ 303.0788, found 303.0798.

*4.1.2.2. 3-((2-Oxo-2-(p-tolyl)ethyl)amino)benzenesulfonamide (**17b**).* Yield 68 mg (18%). Beige amorphous solid. 1H NMR (400 MHz, DMSO-d_6) δ 7.97 (d, J = 7.8 Hz, 2H, ArH), 7.38 (d, J = 7.8 Hz, 2H, ArH), 7.23 (t, J = 7.9 Hz, 1H, ArH), 7.15 (s, 2H, NH2), 7.11 (s, 1H, ArH), 7.01 (d, J = 7.5 Hz, 1H, ArH), 6.89–6.79 (m, 1H, ArH), 6.35 (t, J = 5.3 Hz, 1H, NH), 4.69 (d, J = 5.4 Hz, 2H, CH2), 2.40 (s, 3H, Me). 13C NMR (101 MHz, DMSO-d_6) δ 196.18, 149.03, 145.23, 144.52, 133.06, 129.81, 129.66, 128.44, 115.79, 113.36, 109.43, 49.97, 21.69. HRMS (ESI) m/z [M − H]+ calculated for C15H15N2O3S+ 303.0788, found 303.0798.

*4.1.2.3. 4-((2-(4-Methoxyphenyl)-2-oxoethyl)amino)benzenesulfonamide (**17c**).* Yield 88 mg (24%). Beige solid, m.p. 207.8–208.8 °C. 1H NMR (400 MHz, DMSO-d_6) δ 8.05 (d, J = 8.7 Hz, 2H, ArH), 7.51 (d, J = 8.6 Hz, 2H, ArH), 7.07 (d, J = 8.7 Hz, 2H, ArH), 6.93 (s, 2H, NH2), 6.73 (d, J = 8.5 Hz, 2H, ArH), 4.69 (s, 2H, CH2), 3.85 (s, 3H, OMe).13C NMR (101 MHz, DMSO-d_6) δ 194.76, 163.96, 151.48, 131.04, 130.72, 128.33, 127.66, 114.49, 111.88, 56.07, 49.49. HRMS (ESI) m/z [M − H]+ calculated for C15H15N2O4S+ 319.0758, found 319.0747.

*4.1.2.4. 3-((2-(4-Methoxyphenyl)-2-oxoethyl)amino)benzenesulfonamide (**17d**).* Yield 24 mg (7%). Beige amorphous solid. 1H NMR (400 MHz, acetone-d6) δ 8.11 (d, J = 8.3 Hz, 2H, ArH), 7.28 (d, J = 9.2 Hz, 2H, ArH), 7.16 (d, J = 7.8 Hz, 1H, ArH), 7.08 (d, J = 8.4 Hz, 2H, ArH), 6.99 (t, J = 8.2 Hz, 1H, ArH), 6.29 (s, 2H, NH2), 5.63 (s, 1H, NH), 4.73 (d, J = 4.8 Hz, 2H, CH2), 3.92 (s, 3H, OMe). 13C NMR (101 MHz, acetone-d6) δ 193.27, 164.15, 148.50, 145.14, 130.14, 130.12, 129.34, 128.26, 116.01, 113.98, 109.66, 55.12, 49.49. HRMS (ESI) m/z [M+H]+ calculated for C15H17N2O4S+ 321.0914, found 321.0904.

*4.1.2.5. 3-((3,3-Dimethyl-2-oxobutyl)amino)benzenesulfonamide (**17e**).* Yield 30 mg (25%). Beige solid, m.p. 157.1–159.0 °C. 1H NMR (400 MHz, CD3OD) δ 7.28 (t, J = 7.9 Hz, 1H, ArH), 7.20–7.15 (m, 1H, ArH), 7.12 (t, J = 2.1 Hz, 1H, ArH), 6.85 (ddd, J = 8.3, 2.5, 1.1 Hz, 1H, ArH), 4.25 (s, 2H, CH2), 1.26 (s, 9H, CH3). 13C NMR (101 MHz, CD3OD) δ 211.93, 148.44, 144.14, 129.22, 116.21, 113.84, 109.01, 47.93, 42.76, 25.38. HRMS (ESI) m/z [M+Na]+ calculated for C12H18N2O3S+ 293.0921, found 293.0930.

*4.1.2.6. N,N-diethyl-2-((4-sulfamoylphenyl)amino)acetamide (**17f**).* Yield 50 mg (25%). White solid, m.p. 189.2–191.4 °C. 1H NMR (400 MHz, DMSO-d_6) δ 7.51 (d, J = 8.8 Hz, 2H, ArH), 6.92 (s, 2H, NH2), 6.71 (d, J = 8.8 Hz, 2H, ArH), 6.28 (t, J = 5.0 Hz, 1H, NH), 3.96 (d, J = 5.1 Hz, 2H, CH2), 3.40–3.29 (m, 4H, CH2–Et), 1.16 (t, J = 7.1 Hz, 3H, CH3), 1.05 (t, J = 7.1 Hz, 3H, CH3). 13C NMR (101 MHz, DMSO-d_6) δ 167.91, 151.32, 131.02, 127.61, 111.86, 44.48, 14.53, 13.46. HRMS (ESI) m/z [M+H]+ calculated for C12H20N3O3S+ 286.1218, found 286.1220.

*4.1.2.7. N,N-diethyl-2-((3-sulfamoylphenyl)amino)acetamide (**17g**).* Yield 197 mg (68%). White solid, m.p. 225.1–226.8 °C. 1H NMR (400 MHz, DMSO-d_6) δ 7.24 (t, J = 7.9 Hz, 1H, ArH), 7.17 (s, 2H, NH2), 7.07 (s, 1H, ArH), 7.02 (d, J = 7.6 Hz, 1H, ArH), 6.84 (d, J = 8.5 Hz, 1H, ArH), 6.04 (t, J = 4.5 Hz, 1H, NH), 3.92 (d, J = 5.2 Hz, 2H, CH2), 3.43–3.24 (m, 4H, CH2–Et), 1.17 (t, J = 7.0 Hz, 3H, CH3), 1.06 (t, J = 7.0 Hz, 3H, CH3). 13C NMR (101 MHz, DMSO-d_6) δ 168.09, 148.97, 145.20, 129.63, 115.89, 113.30, 109.39, 44.69, 14.55, 13.47. HRMS (ESI) m/z [M+Na]+ calculated for C12H19N3O3SNa+ 308.1025, found 308.1039.

*4.1.2.8. Ethyl 2-(4-chlorophenyl)-2-((4-sulfamoylphenyl)amino)acetate (**17h**).* Yield 46 mg (29%). White solid, m.p. 170.0–172.1 °C. 1H NMR (400 MHz, DMSO-d_6) δ 7.56–7.44 (m, 6H, ArH), 7.09 (d, J = 8.0 Hz, 1H, NH), 6.93 (s, 2H, NH2), 6.76 (d, J = 8.8 Hz, 2H, ArH), 5.42 (d, J = 8.0 Hz, 1H, CH), 4.24–4.04 (m, 2H, CH2), 1.14 (t, J = 7.1 Hz, 3H, CH3). 13C NMR (101 MHz, DMSO-d_6) δ 171.24, 149.94, 136.78, 133.29, 132.17, 129.89, 129.12, 127.59, 112.62, 61.75, 58.95, 14.41. HRMS (ESI) m/z [M+H]+ calculated for C16H18ClN2O4S+ 369.0677, found 369.0670.

*4.1.2.9. Ethyl 2-(3,4-dimethoxyphenyl)-2-((4-sulfamoylphenyl)amino)acetate (**17i**).* Yield 61 mg (41%). Beige amorphous solid. 1H NMR (400 MHz, CDCl3) δ 7.66–7.57 (m, 2H, ArH), 6.99 (dd, J = 8.2, 2.1 Hz, 1H, ArH), 6.94 (d, J = 2.1 Hz, 1H, ArH), 6.82 (d, J = 8.3 Hz, 1H, ArH), 6.53 (d, J = 8.9 Hz, 2H, ArH), 5.53 (d, J = 5.8 Hz, 1H, NH), 5.06–4.95 (m, 3H, NH2, CH), 4.18 (ddq, J = 35.4, 10.8, 7.1 Hz, 2H, CH2), 3.83 (s, 6H, OMe), 1.21 (t, J = 7.1 Hz, 3H, CH3). 13C NMR (101 MHz, CDCl3) δ 171.34, 149.41, 149.30, 149.23, 130.11, 128.82, 128.30, 119.65, 112.63, 111.40, 109.94, 62.18, 59.77, 55.97, 55.89, 14.03. HRMS (ESI) m/z [M+Na]+ calculated for C18H22N2O6SNa+ 417.1095, found 417.1091.

*4.1.2.10. 4-((2-(4-(4-Chlorobenzyl)piperazin-1-yl)-2-oxoethyl)amino)benzenesulfonamide (**17j**).* Yield 67 mg (44%). Beige amorphous solid. 1H NMR (400 MHz, DMSO-d_6) δ 7.51 (d, J = 8.8 Hz, 2H, ArH), 7.40 (d, J = 8.5 Hz, 2H, ArH), 7.35 (d, J = 8.6 Hz, 2H, ArH), 6.92 (s, 2H, NH2), 6.71 (d, J = 8.9 Hz, 2H, ArH), 6.30 (t, J = 5.2 Hz, 1H, NH), 3.98 (d, J = 5.2 Hz, 2H, CH2), 3.51 (s, 6H, CH2, CH2-piperazine), 2.37 (d, J = 31.6 Hz, 4H, CH2-piperazine). 13C NMR (101 MHz, DMSO-d_6) δ 167.59, 151.32, 137.42, 132.03, 131.13, 131.05, 128.67, 127.60, 111.86, 61.35, 53.08, 52.59, 44.56, 44.43, 41.93. HRMS (ESI) m/z [M+H]+ calculated for C19H24ClN4O3S+ 423.1253, found 423.1252.

*4.1.2.11. 3-((2-(4-(4-Chlorobenzyl)piperazin-1-yl)-2-oxoethyl)amino)benzenesulfonamide (**17k**).* Yield 48 mg (41%). Beige solid, m.p. 239.1–240.9 °C. 1H NMR (400 MHz, DMSO-d_6) δ 7.39 (d, J = 8.2 Hz, 2H, ArH), 7.34 (d, J = 8.4 Hz, 2H, ArH), 7.22 (t, J = 7.9 Hz, 1H, ArH), 7.15 (s, 2H, NH2), 7.06 (s, 1H, ArH), 7.00 (d, J = 7.5 Hz, 1H, ArH), 6.86–6.78 (m, 1H, ArH), 6.06 (t, J = 5.0 Hz, 1H, NH), 3.94 (d, J = 5.0 Hz, 2H, CH2), 3.50 (s, 6H, CH2, CH2-piperazine), 2.37 (d, J = 34.4 Hz, 4H, CH2-piperazine). 13C NMR (101 MHz, DMSO-d_6) δ 167.80, 148.95, 145.20, 137.44, 132.03, 131.12, 129.63, 128.68, 115.84, 113.33, 109.43, 61.36, 53.08, 52.60, 44.78, 44.48, 41.94. HRMS (ESI) m/z [M+H]+ calculated for C19H24ClN4O3S+ 423.1253, found 423.1252.

*4.1.2.12. 4-((2-Oxocycloheptyl)amino)benzenesulfonamide (**17l**).* Yield 80 mg (20%). Beige solid, m.p. 153.9–155.7 °C. 1H NMR (400 MHz, (CD3)2CO) δ 7.62 (d, J = 8.8 Hz, 2H, ArH), 6.71 (d, J = 8.8 Hz, 2H, ArH), 6.15 (s, 2H, NH2), 5.86 (s, 1H, NH), 4.47–4.39 (m, 1H, CH-cycloheptanone), 2.69 (dt, J = 16.8, 4.7 Hz, 1H, CH2-cycloheptanone), 2.48 (ddd, J = 16.8, 10.2, 4.5 Hz, 1H, CH2-cycloheptanone), 2.14–2.05 (m, 2H, CH2-cycloheptanone), 1.98–1.72 (m, 6H, CH2-cycloheptanone), 1.55 (dtd, J = 14.1, 9.6,

4.0 Hz, 1H, CH2-cycloheptanone), 1.47–1.34 (m, 1H, CH2-cycloheptanone).13C NMR (101 MHz, (CD3)2CO) δ 209.41, 149.69, 131.31, 127.87, 111.86, 61.05, 41.05, 31.25, 26.98, 23.19. HRMS (ESI) *m/z* [M − H]+ calculated for C13H17N2O3S+ 281.0944, found 281.0954.

*4.1.2.13. Dimethyl 2-((4-sulfamoylphenyl)amino)malonate (**19a**).* Yield 63 mg (33%). Beige solid, m.p. 208.7–210.0 °C. 1H NMR (400 MHz, acetone-d6) δ 7.66 (d, *J* = 14.3 Hz, 2H, ArH), 6.91–6.80 (m, 2H, ArH), 6.23 (s, 2H, NH2), 6.17 (d, *J* = 8.0 Hz, 1H, NH), 5.07 (d, *J* = 8.1 Hz, 1H, CH), 3.79 (s, 6H, OMe).13C NMR (101 MHz, acetone-d6) δ 168.40, 150.10, 133.93, 128.72, 113.15, 60.29, 53.43. HRMS (ESI) *m/z* [M+Na]+ calculated for C11H14N2O6SNa+ 325.0470, found 325.0465.

*4.1.2.14. Diethyl 2-((4-sulfamoylphenyl)amino)malonate (**19b**).* Yield 28 mg (35%). White solid, m.p. 146.4–147.4 °C. 1H NMR (400 MHz, DMSO-d_6) δ 7.53 (d, *J* = 8.7 Hz, 2H, ArH), 6.97 (d, *J* = 6.9 Hz, 3H, NH2, NH), 6.80 (d, *J* = 8.8 Hz, 2H, ArH), 5.16 (d, *J* = 8.6 Hz, 1H, CH), 4.20 (dtq, *J* = 10.3, 6.9, 3.4 Hz, 4H, CH2), 1.21 (t, *J* = 7.1 Hz, 6H, CH3). 13C NMR (101 MHz, DMSO-d_6) δ 167.67, 149.68, 132.60, 127.65, 112.49, 62.30, 59.80, 14.34. HRMS (ESI) *m/z* [M+Na]+ calculated for C13H18N2O6SNa+ 353.0784, found 353.0778.

*4.1.2.15. Diisopropyl 2-((4-sulfamoylphenyl)amino)malonate (**19c**).* Yield 30 mg (18%). White amorphous solid. 1H NMR (400 MHz, DMSO-d_6) δ 7.53 (d, *J* = 8.8 Hz, 2H, ArH), 6.97 (s, 2H, NH2), 6.89 (d, *J* = 8.5 Hz, 1H, NH), 6.80 (d, *J* = 8.9 Hz, 2H, ArH), 5.12–4.92 (m, 3H, CH, CH-i-Pr), 1.24 (d, *J* = 6.2 Hz, 6H, CH3), 1.20 (d, *J* = 6.3 Hz, 6H, CH3). 13C NMR (101 MHz, DMSO-d_6) δ 167.17, 149.61, 132.11, 127.70, 112.57, 79.24, 78.91, 78.59, 70.54, 54.90, 21.67, 21.56. HRMS (ESI) *m/z* [M+Na]+ calculated for C15H22N2O6SNa+ 381.1102, found 381.1091.

*4.1.2.16. Bis(2-methoxyethyl) 2-((4-sulfamoylphenyl)amino)malonate (**19d**).* Yield 112 mg (70%); white solid, m.p. 113.1–115.4 °C. 1H NMR (400 MHz, DMSO-d_6) δ 7.54 (d, *J* = 8.8 Hz, 2H, ArH), 7.00 (d, *J* = 8.0 Hz, 3H, NH, NH2), 6.82 (d, *J* = 8.9 Hz, 2H, ArH), 5.23 (d, *J* = 8.6 Hz, 1H, CH), 4.32–4.23 (m, 4H, CH2), 3.59–3.46 (m, 4H, CH2), 3.26 (s, 6H, OMe). 13C NMR (101 MHz, DMSO-d_6) δ 167.63, 149.62, 132.76, 127.59, 112.56, 69.90, 65.28, 59.71, 58.54. HRMS (ESI) *m/z* [M − H]+ calculated for C15H21N2O8S+ 389.1008, found 389.1013.

*4.1.2.17. Methyl 4-methoxy-3-oxo-2-((4-sulfamoylphenyl)amino) butanoate (**16e**).* Yield 21 mg (12%). White amorphous solid,. 1H NMR (400 MHz, DMSO-d_6) δ 7.53 (d, *J* = 8.8 Hz, 2H, ArH), 6.96 (s, 2H, NH2), 6.70 (d, *J* = 8.9 Hz, 3H, ArH, NH), 4.54 (td, *J* = 8.0, 5.5 Hz, 1H, NH), 3.65 (s, 3H, OMe), 3.62 (s, 3H, OMe), 2.92 (dd, *J* = 16.4, 5.6 Hz, 1H, CH2), 2.81 (dd, *J* = 16.4, 7.5 Hz, 1H, CH2). 13C NMR (101 MHz, DMSO-d_6) δ 172.49, 170.93, 150.49, 132.00, 127.78, 112.08, 52.66, 52.33, 52.22, 36.76. HRMS (ESI) *m/z* [M+H]+ calculated for C12H16N2O6S+ 317.0812, found 317.0802.

*4.1.2.18. Ethyl 3-oxo-3-phenyl-2-((4-sulfamoylphenyl)amino)propanoate (**19f**).* Yield 111 mg (66%). Beige amorphous solid. 1H NMR (400 MHz, CDCl3) δ 13.03 (s, 0.06H, OH), 8.16 (dd, *J* = 8.4, 1.2 Hz, 2H, ArH), 7.77 (d, *J* = 8.8 Hz, 2H, ArH), 7.76–7.65 (m, 1.28H, ArH), 7.56 (t, *J* = 7.8 Hz, 2H, ArH), 7.45–7.37 (m, 0.10H, ArH), 7.39–7.31 (m, 0.23H, ArH), 6.78 (d, *J* = 8.9 Hz, 2H, ArH), 6.68 (d, *J* = 8.8 Hz, 0.17H, ArH), 5.84 (d, *J* = 7.1 Hz, 1H, NH), 5.71 (d, *J* = 7.2 Hz, 1H, CH), 5.14 (s, 0.07H, NH2), 4.75 (s, 2H, NH2), 4.27 (q, *J* = 7.1 Hz, 0.28H, CH2), 4.18 (q, *J* = 7.1 Hz, 2H, CH2), 1.21 (t, *J* = 7.1 Hz, 0.33H, CH3), 1.12 (t, *J* = 7.1 Hz, 3H, CH3). 13C NMR (101 MHz, CDCl3) δ 190.77, 167.38, 149.08, 134.70, 133.77, 130.73, 129.26, 128.95, 128.70, 112.85, 62.73, 62.64, 13.85. More number of proton peaks are due to the keto-enol tautomerism (17:1). HRMS (ESI) *m/z* [M+Na]+ calculated for C17H18N2O5SNa+ 385.0828, found 385.0829.

*4.1.2.19. Ethyl 3-oxo-3-phenyl-2-((3-sulfamoylphenyl)amino)propanoate (**19g**).* Yield 74 mg (23%). White amorphous solid. 1H NMR (400 MHz, (CD3)2CO) δ 8.20–8.14 (m, 2H, ArH), 7.76–7.68 (m, 1H, ArH), 7.59 (t, *J* = 7.7 Hz, 2H, ArH), 7.42–7.36 (m, 1H, ArH), 7.32 (t, *J* = 7.9 Hz, 1H, ArH), 7.25–7.18 (m, 1H, ArH), 7.06 (dd, *J* = 8.1, 1.6 Hz, 1H, ArH), 6.43 (s, 2H, NH2), 6.14 (d, *J* = 8.5 Hz, 1H, NH), 6.02 (d, *J* = 8.4 Hz, 1H, CH), 4.14 (q, *J* = 7.1 Hz, 2H, CH2), 1.09 (t, *J* = 7.1 Hz, 3H, CH3).13C NMR (101 MHz, (CD3)2CO) δ 193.09, 168.84, 147.80, 146.09, 135.52, 135.05, 130.50, 129.99, 129.68, 117.20, 116.14, 11.57, 63.40, 62.56, 14.21. HRMS (ESI) *m/z* [M+Na]+ calculated for C17H18N2O5SNa+ 385.0833, found 385.0829.

*4.1.2.20. Ethyl 3-(4-methoxyphenyl)-3-oxo-2-((4-sulfamoylphenyl) amino)propanoate (**19h**).* Yield 30 mg (19%). White amorphous solid. 1H NMR (400 MHz, (CD3)2CO) δ 8.24–8.16 (m, 2H, ArH), 7.75–7.64 (m, 2H, ArH), 7.15–7.08 (m, 2H, ArH), 6.96 (d, *J* = 8.8 Hz, 2H, ArH), 6.32 (d, *J* = 8.2 Hz, 1H, NH), 6.23 (s, 2H, NH2), 6.06–6.02 (m, 1H, CH), 4.16 (q, *J* = 7.1 Hz, 2H, CH2), 3.95 (s, 3H, OMe), 1.12 (t, *J* = 7.1 Hz, 3H, CH3). 13C NMR (101 MHz, (CD3)2CO) δ 189.98, 167.91, 164.65, 149.47, 132.78, 131.66, 127.82, 127.29, 114.02, 112.48, 61.78, 61.65, 55.24, 13.35. HRMS (ESI) *m/z* [M+Na]+ calculated for C18H20N2O6SNa+ 415.0933, found 415.0934.

*4.1.2.21. Ethyl 3-(4-methoxyphenyl)-3-oxo-2-((3-sulfamoylphenyl) amino)propanoate (**19i**).* Yield 84 mg (28%). White amorphous solid. 1H NMR (400 MHz, CDCl3) δ 8.16 (d, *J* = 8.3 Hz, 2H, ArH), 7.42–7.24 (m, 3H, ArH), 7.01 (d, *J* = 8.3 Hz, 2H, ArH), 6.93 (d, *J* = 6.7 Hz, 1H, ArH), 5.66 (s, 2H, CH, NH), 4.84 (s, 2H, NH2), 4.17 (q, *J* = 6.4 Hz, 2H, CH2), 3.93 (s, 3H, OMe), 1.14 (t, *J* = 6.8 Hz, 3H, CH3). 13C NMR (101 MHz, CDCl3) δ 189.19, 168.00, 164.75, 146.33, 143.01, 131.79, 130.25, 126.77, 117.78, 116.05, 114.16, 110.53, 77.22, 62.52, 55.64, 13.91. HRMS (ESI) *m/z* [M+H]+ calculated for C18H21N2O6S+ 393.1104, found 393.1115.

*4.1.2.22. Methyl 3-(2-methoxyphenyl)-3-oxo-2-((4-sulfamoylphenyl) amino)propanoate (**19j**).* Yield 100 mg (31%). Beige solid, m.p. 203.6–205 °C. 1H NMR (400 MHz, CD3OD) δ 7.84 (d, *J* = 8.8 Hz, 2H, ArH), 7.75 (t, *J* = 9.6 Hz, 2H, ArH), 7.33 (t, *J* = 7.3 Hz, 2H, ArH), 7.02 (d, *J* = 8.3 Hz, 1H, ArH), 6.99–6.93 (m, 1H, ArH), 3.85 (s, 3H, OMe), 3.75 (s, 3H, OMe). 13C NMR (101 MHz, CD3OD) δ 169.89, 167.56, 157.12, 141.85, 138.67, 129.14, 128.87, 126.81, 122.32, 120.29, 119.19, 110.48, 54.77, 51.69. HRMS (ESI) *m/z* [M − H]+ calculated for C17H17N2O6S+ 377.0806, found 377.0802.

*4.1.2.23. Ethyl 3-methyl-2-((4-sulfamoylphenyl)carbamoyl)butanoate (**20a**).* Yield 135 mg (38%). White amorphous solid. 1H NMR (400 MHz, CD3OD) δ 7.87 (d, *J* = 8.8 Hz, 2H, ArH), 7.77 (d, *J* = 8.9 Hz, 2H, ArH), 4.22 (qd, *J* = 7.1, 1.4 Hz, 2H, CH2), 3.21 (d, *J* = 9.8 Hz, 1H, CH), 2.47 (ddt, *J* = 13.4, 9.9, 6.7 Hz, 1H, CH- i-Pr), 1.28 (t, *J* = 7.1 Hz, 3H, CH3), 1.04 (dd, *J* = 12.2, 6.7 Hz, 6H, CH3-i-Pr). 13C NMR (101 MHz, CD3OD) δ 169.42, 168.00, 141.60, 138.80, 126.83, 119.28, 61.08, 60.97, 29.09, 19.61, 19.06, 13.05. HRMS (ESI) *m/z* [M+Na]+ calculated for C14H20N2O5SNa+ 351.0998, found 351.0985.

*4.1.2.24. Ethyl 3-methyl-2-((3-sulfamoylphenyl)carbamoyl)butanoate (**20b**).* Yield 135 mg (38%). Dirty pink amorphous solid. 1H NMR (400 MHz, (CD3)2CO), 9.60 (s, 1H, NH), 8.31 (s, 1H, ArH), 7.79 (d, *J* = 8.0 Hz, 1H, ArH), 7.62 (d, *J* = 7.8 Hz, 1H, ArH), 7.49 (t, *J* = 7.9 Hz, 1H, ArH), 6.63 (s, 2H, NH2), 4.16 (tt, *J* = 10.6, 5.3 Hz, 2H, CH2), 3.19 (d, *J* = 9.6 Hz, 1H, CH), 2.46 (ddt, *J* = 13.3, 9.0, 6.6 Hz, 1H, CH-i-Pr), 1.22 (t, *J* = 7.1 Hz, 3H, CH3), 1.01 (d, *J* = 6.7 Hz, 6H, CH3-i-Pr). 13C

NMR (101 MHz, (CD3)2CO) δ 170.05, 167.47, 145.83, 140.21, 130.28, 123.32, 122.04, 117.83, 62.17, 61.59, 20.89, 20.47, 14.46. HRMS (ESI) *m/z* [M+Na]+ calculated for C14H20N2O5SNa+ 351.0985, found 351.0985.

*4.1.2.25. Ethyl 3-oxo-2-phenyl-3-((4-sulfamoylphenyl)amino)propanoate (**20c**).* Yield 163 mg (41%). Beige amorphous solid. 1H NMR (400 MHz, DMSO-d_6) δ 10.68 (s, 1H, NH), 7.76 (d, J = 8.8 Hz, 2H, ArH), 7.71 (d, J = 8.7 Hz, 2H, ArH), 7.46–7.31 (m, 5H), 7.25 (s, 2H, NH2), 4.93 (s, 1H, CH), 4.15 (q, J = 7.0 Hz, 2H, CH2), 1.18 (t, J = 7.1 Hz, 3H, CH3). 13C NMR (101 MHz, DMSO-d_6) δ 168.28, 166.27, 141.48, 138.90, 133.88, 127.79, 126.77, 118.87, 61.13, 58.32, 13.97. HRMS (ESI) *m/z* [M+Na]+ calculated for C17H18N2O5SNa+ 385.0829, found 385.0829.

*4.1.2.26. 2-Benzoyl-3-methyl-N-(4-sulfamoylphenyl)butanamide (**20d**).* Yield 51 mg (32%). White solid, m.p. 211.4–212.9 °C. 1H NMR (400 MHz, DMSO-d_6) δ 10.63 (s, 1H, NH), 8.07 (d, J = 7.3 Hz, 2H, ArH), 7.75 (d, J = 8.6 Hz, 2H, ArH), 7.69 (m, J = 9.0 Hz, 3H, ArH), 7.56 (d, J = 7.7 Hz, 2H, ArH), 7.23 (s, 2H, NH2), 4.37 (d, J = 9.4 Hz, 1H, CH), 2.57 (dt, J = 9.1, 6.7 Hz, 1H, CH-i-Pr), 1.00 (d, J = 6.8 Hz, 3H, CH3), 0.93 (d, J = 6.6 Hz, 3H, CH3). 13C NMR (101 MHz, DMSO-d_6) δ 195.13, 167.65, 141.84, 139.38, 137.14, 134.04, 129.38, 128.61, 127.19, 119.50, 62.82, 29.14, 21.61, 20.38. HRMS (ESI) *m/z* [M+Na]+ calculated for C18H20N2O4SNa+ 383.1037, found 383.1036.

*4.1.2.27. 2-Benzoyl-3-methyl-N-(3-sulfamoylphenyl)butanamide (**20e**).* Yield 65 mg (41%). White amorphous solid. 1H NMR (400 MHz, acetone-d6) δ 14.93 (s, 0.01H, OH), 9.73 (s, 0.38H, NH), 9.63 (s, 1H, NH), 8.25 (s, 1,2H, ArH), 8.13 (d, J = 7.4 Hz, 1H, ArH), 8.09 (d, J = 7.3 Hz, 0.19H, ArH), 7.79 (d, J = 8.1 Hz, 1.59H), 7.53–7.67 (m, 6.24H, ArH), 7.47 (t, J = 7.9 Hz, 2.08H, ArH), 7.31–7.40 (m, 1.21H, ArH), 6.59 (s, 2H, NH2), 4.37 (d, J = 9.6 Hz, 1H, CH), 2.92 (dt, J = 13.7, 6.9 Hz, 0.28H, CH), 2.72 (dqd, J = 13.4, 6.7, 3.1 Hz, 1H, CH), 1.10 (d, J = 6.7 Hz, 3.31H, CH3), 1.05 (d, J = 6.9 Hz, 0.65H, CH3), 0.98 (d, J = 3.0 Hz, 3H, CH3). 13C NMR (101 MHz, acetone-d6) δ 196.46, 167.75, 145.76, 140.11, 138.22, 134.37, 130.38, 130.26, 129.72, 129.67, 129.32, 129.28, 129.20, 123.41, 123.31, 122.09, 117.90, 117.81, 65.26, 64.47, 30.59, 21.62, 21.47, 20.54, 18.93, 18.80. Higher number of proton peaks is attributed to the keto-enol tautomerism (7:1). HRMS (ESI) *m/z* [M+Na]+ calculated for C18H20N2O4SNa+ 383.1028, found 383.1036.

*4.1.2.28. 3-(4-Chlorophenyl)-2-methyl-3-oxo-N-(4-sulfamoylphenyl) propenamide (**20f**).* Yield 44 mg (28%). White solid, m.p. 223.6–225.1 °C. 1H NMR (400 MHz, DMSO-d_6) δ 10.63 (s, 1H, NH), 8.00 (d, J = 8.6 Hz, 2H, ArH), 7.75 (d, J = 8.8 Hz, 2H, ArH), 7.69 (d, J = 8.9 Hz, 2H, ArH), 7.63 (d, J = 8.7 Hz, 2H, ArH), 7.24 (s, 2H, NH2), 4.64 (q, J = 6.8 Hz, 1H, CH), 1.39 (d, J = 6.9 Hz, 3H, Me). 13C NMR (101 MHz, DMSO-d_6) δ 195.91, 169.91, 142.20, 139.16, 138.77, 135.00, 130.51, 129.47, 127.19, 119.29, 50.07, 14.54. HRMS (ESI) *m/z* [M − H]+ calculated for C16H14ClN2O4S+ 365.0373, found 365.0357.

*4.1.2.29. 4-((4-(4-Chlorobenzyl)-2,5-dioxo-1-(p-tolyl)-2,5-dihydro-1H-pyrrol-3-yl)amino)benzenesulfonamide (**22a**).* Yield 100 mg (71%). Yellow solid, m.p. 260.0–261.9 °C. 1H NMR (400 MHz, (CD3) 2CO) δ 8.62 (s, 1H, NH), 7.88–7.79 (m, 2H, ArH), 7.32 (m, 2H, ArH), 7.28 (d, J = 8.3 Hz, 2H, ArH), 7.26–7.21 (m, 2H, ArH), 7.14–7.09 (m, 2H, ArH), 6.82 (d, J = 8.4 Hz, 2H, ArH), 6.60 (s, 2H, NH2), 3.65 (s, 2H, CH2), 2.37 (s, 3H, Me). 13C NMR (101 MHz, (CD3)2CO) δ 172.66, 167.86, 142.90, 140.72, 139.93, 138.21, 137.81, 132.02, 130.89, 130.67, 130.08, 129.01, 127.81, 126.85, 123.56, 105.18, 28.91, 21.06. HRMS (ESI) *m/z* [M+H]+ calculated for C24H20ClN3O4S+ 480.0790, found 480.0790.

*4.1.2.30. 3-((4-(4-Chlorobenzyl)-2,5-dioxo-1-(p-tolyl)-2,5-dihydro-1H-pyrrol-3-yl)amino)benzenesulfonamide (**22b**).* Yield 96 mg (69%). Yellow solid, m.p. 149.3–151.6 °C. 1H NMR (400 MHz, (CD3) 2CO) δ 8.59 (s, 1H, NH), 7.71–7.62 (m, 2H, ArH), 7.37–7.23 (m, 6H, ArH), 7.10–7.03 (m, 2H, ArH), 6.77 (d, J = 8.4 Hz, 2H, ArH), 6.72 (s, 2H, NH2), 3.62 (s, 2H, CH2), 2.37 (s, 3H, Me). 13C NMR (101 MHz, (CD3)2CO) δ 13C NMR (101 MHz, Acetone) δ 172.79, 167.86, 145.71, 140.12, 138.42, 137.78, 131.92, 130.96, 130.56, 130.26, 130.08, 128.94, 127.51, 126.86, 122.98, 121.43, 103.65, 28.70, 21.07. HRMS (ESI) *m/z* [M+H]+ calculated for C24H21ClN3O4S+ 482.0938, found 482.0936.

*4.1.2.31. 4-((4-(2-Methoxybenzyl)-2,5-dioxo-1-phenyl-2,5-dihydro-1H-pyrrol-3-yl)amino)benzenesulfonamide (**22c**).* Yield 148 mg (51%). Yellow amorphous solid. 1H NMR (400 MHz, DMSO-d_6) δ9.51 (s, 1H, NH), 7.62 (d, J = 8.6 Hz, 2H, ArH), 7.52–7.47 (m, 2H, ArH), 7.39 (dd, J = 15.5, 7.5 Hz, 3H, ArH), 7.24 (s, 2H, NH2), 7.10 (dd, J = 12.2, 8.9 Hz, 3H, ArH), 6.89 (d, J = 6.6 Hz, 1H, ArH), 6.76 (dd, J = 17.7, 7.9 Hz, 2H, ArH), 3.62 (s, 3H, OMe), 3.51 (s, 2H, CH2). 13C NMR (101 MHz, DMSO-d_6) δ 171.32, 166.71, 156.60, 142.31, 139.13, 138.33, 132.08, 128.79, 128.59, 127.33, 127.27, 126.44, 126.14, 125.34, 121.05, 119.97, 110.17, 105.66, 64.91, 55.08, 45.76, 23.15, 15.16, 8.68. HRMS (ESI) *m/z* [M+H]+ calculated for C24H22N3O5S+ 464.1273, found 464.1275.

4.2. Carbonic anhydrase inhibition assay

An Applied Photophysics stopped-flow instrument has been used for assaying the CA catalyzed CO_2 hydration activity [52]. Phenol red (at a concentration of 0.2 mM) has been used as indicator, working at the absorbance maximum of 557 nm, with 20 mM Hepes (pH 7.5) as buffer, and 20 mM Na_2SO_4 (for maintaining constant the ionic strength), following the initial rates of the CA-catalyzed CO_2 hydration reaction for a period of 10–100 s.15 The CO_2 concentrations ranged from 1.7 to 17 mM for the determination of the kinetic parameters and inhibition constants. For each inhibitor at least six traces of the initial 5–10% of the reaction have been used for determining the initial velocity. The uncatalyzed rates were determined in the same manner and subtracted from the total observed rates. Stock solutions of inhibitor (0.1 mM) were prepared in distilled–deionized water and dilutions up to 0.01 nM were done thereafter with the assay buffer. Inhibitor and enzyme solutions were preincubated together for 15 min at room temperature prior to assay, in order to allow for the formation of the E–I complex. The inhibition constants were subsequently obtained by nonlinear least-squares methods using PRISM 3 and the Cheng–Prusoff equation, as reported earlier, and represent the mean from at least three different determinations. All CA isoforms were recombinant ones obtained in-house as reported earlier [78–81].

4.3. Cell culture

MCF7 breast carcinoma cells, MDA-MB-231 mammary gland/breast cancer cell, WI-26 VA4 lung epithelial-like cells were purchased from the ATCC. MCF7 cells were maintained in Advanced MEM (Gibco, UK) supplemented with 5% fetal bovine serum (FBS, Gibco, UK), penicillin (100 UI mL^{-1}), streptomycin (100 μg mL^{-1}), human recombinant insulin (10 μg mL^{-1}, Capricorn Scientific, Germany), and GlutaMax (1.87 mM, Gibco, UK). MDA-MB-231 cells were maintained in Advanced DMEM/F12 (Gibco, UK) supplemented with 5% fetal bovine serum (FBS, Gibco, UK), penicillin (100 UI mL^{-1}), streptomycin (100 μg mL^{-1}), and GlutaMax (2.5 mM, Gibco, UK). WI-26 VA4 cells were maintained in Advanced MEM (Gibco, UK) supplemented with 5% fetal bovine serum (FBS, Gibco,

UK), penicillin (100 UI mL^{-1}), streptomycin (100 μg mL^{-1}), and GlutaMax (1.87 mM, Gibco, UK). All cells line cultivation under a humidified atmosphere of 95% air/5% CO_2 at 37 °C. Subconfluent monolayers, in the log growth phase, were harvested by a brief treatment with TrypLE Express solution (Gibco, UK) in phosphate buffered saline (PBS, Capricorn Scientific, Germany) and washed three times in serum-free PBS. The number of viable cells was determined by trypan blue exclusion.

4.3. Antiproliferative assay (end point)

The effects of the synthesized compounds on cell viability were determined using the MTT colorimetric test. All examined cells were diluted with the growth medium (or medium containing 100 μM $CoCl_2$ for chemically-induced hypoxia) to 3.5 × 104 cells per mL and the aliquots (7 × 103 cells per 200 μL) were placed in individual wells in 96-multiplates (Eppendorf, Germany) and incubated for 24 h. The next day the cells were then treated with synthesized compounds separately at 100 μM concentration and incubated for 72 h at 37 °C in 5% CO_2 atmosphere. Each compound was tested in triplicate. After incubation, the cells were then treated with 40 μL MTT solution (3-(4,5-dimethylthiazol-2-yl)-2,5-diphenyltetrazolium bromide, 5 mg mL-1 in PBS) and incubated 4 h. After an additional 4 h incubation, the medium with MTT was removed and DMSO (150 μL) was added to dissolve the crystals formazan. The plates were shaken for 10 min. The optical density of each well was determined at 560 nm using a microplate reader GloMax Multi+ (Promega, USA). Each of the tested compounds was evaluated for cytotoxicity in three separate experiments.

4.4. MTT assay

All examined cells were diluted with the growth medium (or medium containing 100 μM $CoCl_2$ for chemically-induced hypoxia) to 3.5 × 104 cells per mL and the aliquots (7 × 103 cells per 200 μL) were placed in individual wells in 96-multiplates (Eppendorf, Germany) and incubated for 24 h. Triplicate wells were treated with test compounds starting at 200.0 μM concentration and diluted 11 at various concentrations or DMSO (Sigma, USA) as control with final concentration 0.1%. Plates were incubated for 72 h at 37 °C in 5% CO_2 atmosphere. After incubation, the cells were then treated with 40 μL MTT solution (3-(4,5-dimethylthiazol-2-yl)-2,5-diphenyltetrazolium bromide, 5 mg mL-1 in PBS) and incubated 4 h. After an additional 4 h incubation, the medium with MTT was removed and DMSO (150 μL) was added to dissolve the crystals formazan. The plates were shaken for 10 min. The optical density of each well was determined at 560 nm using a microplate reader GloMax Multi+ (Promega, USA). Each of the tested compounds was evaluated for cytotoxicity in three separate experiments.

Declaration of competing interest

The authors declare that they have no known competing financial interests or personal relationships that could have appeared to influence the work reported in this paper.

Acknowledgements

This research was supported by the Russian Federation Government Megagrant 14.W03.031.0025. We are grateful to the Centre for Chemical Analysis and Materials Research of Saint Petersburg State University Research Park for the high-resolution mass-spectrometry data. T.S. is grateful to the Russian Foundation for Basic Research (project grant 19–33-90017).

Appendix A. Supplementary data

Supplementary data to this article can be found online at https://doi.org/10.1016/j.ejmech.2021.113352.

References

[1] C.T. Supuran, Structure and function of carbonic anhydrases, Biochem. J. 473 (2016) 2023–2032, https://doi.org/10.1042/BCJ20160115.
[2] C.D. Boone, M. Pinard, R. McKenna, D. Silverman, Catalytic mechanism of α-class carbonic anhydrases: CO2 hydration and proton transfer, Subcell. Biochem. 75 (2014) 31–52, https://doi.org/10.1007/978-94-007-7359-2_3.
[3] C.T. Supuran, C. Capasso, An overview of the bacterial carbonic anhydrases, Metabolites 7 (2017) 56, https://doi.org/10.3390/metabo7040056.
[4] A. Angeli, M. Pinteala, S.S. Maier, S. Del Prete, C. Capasso, B.C. Simionescu, C.T. Supuran, Inhibition of α-, β-, γ-, δ-, ζ- and η-class carbonic anhydrases from bacteria, fungi, algae, diatoms and protozoans with famotidine, J. Enzym. Inhib. Med. Chem. 34 (2019) 644–650, https://doi.org/10.1080/14756366.2019.1571273.
[5] E. Berrino, M. Bozdag, S. Del Prete, F.A.S. Alasmary, L.S. Alqahtani, Z. AlOthman, C. Capasso, C.T. Supuran, Inhibition of α-, β-, γ-, and δ-carbonic anhydrases from bacteria and diatoms with *N′* -aryl- *N* -hydroxy-ureas, J. Enzym. Inhib. Med. Chem. 33 (2018) 1194–1198, https://doi.org/10.1080/14756366.2018.1490733.
[6] V. De Luca, A. Petreni, A. Nocentini, A. Scaloni, C.T. Supuran, C. Capasso, Effect of sulfonamides and their structurally related derivatives on the activity of ι-carbonic anhydrase from burkholderia territorii, Int. J. Mol. Sci. 22 (2021) 1–13, https://doi.org/10.3390/ijms22020571.
[7] S. Del Prete, V. De Luca, G. De Simone, C.T. Supuran, C. Capasso, Cloning, expression and purification of the complete domain of the η-carbonic anhydrase from Plasmodium falciparum, J. Enzym. Inhib. Med. Chem. 31 (2016) 54–59, https://doi.org/10.1080/14756366.2016.1217856.
[8] R. McKenna, C.T. Supuran, Carbonic anhydrase inhibitors drug design, Subcell. Biochem. 75 (2014) 291–323, https://doi.org/10.1007/978-94-007-7359-2_15.
[9] C.T. Supuran, Structure-based drug discovery of carbonic anhydrase inhibitors, J. Enzym. Inhib. Med. Chem. 27 (2012) 759–772, https://doi.org/10.3109/14756366.2012.672983.
[10] K.M. Gilmour, Perspectives on carbonic anhydrase, Comp. Biochem. Physiol. - A Mol. Integr. Physiol. 157 (2010) 193–197, https://doi.org/10.1016/j.cbpa.2010.06.161.
[11] M.E. McDevitt, L.A. Lambert, Molecular evolution and selection pressure in alpha-class carbonic anhydrase family members, Biochim. Biophys. Acta Protein Proteonomics 1814 (2011) 1854–1861, https://doi.org/10.1016/j.bbapap.2011.07.007.
[12] S.C. Frost, Physiological functions of the alpha class of carbonic anhydrases, Subcell. Biochem. 75 (2014) 9–30, https://doi.org/10.1007/978-94-007-7359-2_2.
[13] R. McKenna, S.C. Frost, Overview of the carbonic anhydrase family, Subcell. Biochem. 75 (2014) 3–5, https://doi.org/10.1007/978-94-007-7359-2_1.
[14] S. Zamanova, A.M. Shabana, U.K. Mondal, M.A. Ilies, Carbonic anhydrases as disease markers, Expert Opin. Ther. Pat. 29 (2019) 509–533, https://doi.org/10.1080/13543776.2019.1629419.
[15] C. Supuran, Carbonic anhydrases as drug targets - an overview, Curr. Top. Med. Chem. 7 (2007) 825–833, https://doi.org/10.2174/156802607780636690.
[16] S. Kalinin, A. Valtari, M. Ruponen, E. Toropainen, A. Kovalenko, A. Nocentini, M. Gureev, D. Dar'in, A. Urtti, C.T. Supuran, M. Krasavin, Highly hydrophilic 1,3-oxazol-5-yl benzenesulfonamide inhibitors of carbonic anhydrase II for reduction of glaucoma-related intraocular pressure, Bioorg. Med. Chem. 27 (2019), https://doi.org/10.1016/j.bmc.2019.115086.
[17] A. Nocentini, C.T. Supuran, Carbonic anhydrase inhibitors for the treatment of neuropathic pain and arthritis, in: Carbon. Anhydrases Biochem. Pharmacol. An Evergr. Pharm. Target, Elsevier, 2019, pp. 367–386, https://doi.org/10.1016/B978-0-12-816476-1.00017-4.
[18] C.T. Supuran, Carbonic anhydrase inhibitors as emerging drugs for the treatment of obesity, Expet Opin. Emerg. Drugs 17 (2012) 11–15, https://doi.org/10.1517/14728214.2012.664132.
[19] A. Scozzafava, C.T. Supuran, Glaucoma and the applications of carbonic anhydrase inhibitors, Subcell. Biochem. 75 (2014) 349–359, https://doi.org/10.1007/978-94-007-7359-2_17.
[20] C.T. Supuran, Carbonic anhydrases: novel therapeutic applications for inhibitors and activators, Nat. Rev. Drug Discov. 7 (2008) 168–181, https://doi.org/10.1038/nrd2467.
[21] C.T. Supuran, Experimental carbonic anhydrase inhibitors for the treatment of hypoxic tumors, J. Exp. Pharmacol. 12 (2020) 603–617, https://doi.org/10.2147/JEP.S265620.
[22] I.S. Ismail, The role of carbonic anhydrase in hepatic glucose production, Curr. Diabetes Rev. 14 (2018) 108–112, https://doi.org/10.2174/1573399812666161214122351.
[23] P. Blandina, G. Provensi, M.B. Passani, C. Capasso, C.T. Supuran, Carbonic anhydrase modulation of emotional memory. Implications for the treatment of cognitive disorders, J. Enzym. Inhib. Med. Chem. 35 (2020) 1206–1214,

https://doi.org/10.1080/14756366.2020.1766455.
[24] C.T. Supuran, How many carbonic anhydrase inhibition mechanisms exist? J. Enzym. Inhib. Med. Chem. 31 (2016) 345–360, https://doi.org/10.3109/14756366.2015.1122001.
[25] J.-Y. Winum, J.-L. Montero, A. Scozzafava, C.T. Supuran, Zinc binding functions in the design of carbonic anhydrase inhibitors, in: Drug Des. Zinc-Enzyme Inhib., John Wiley & Sons, Inc., Hoboken, NJ, USA, 2009, pp. 39–72, https://doi.org/10.1002/9780470508169.ch3.
[26] M. Ferraroni, B. Cornelio, J. Sapi, C.T. Supuran, A. Scozzafava, Sulfonamide carbonic anhydrase inhibitors: zinc coordination and tail effects influence inhibitory efficacy and selectivity for different isoforms, Inorg. Chim. Acta. 470 (2018) 128–132, https://doi.org/10.1016/j.ica.2017.03.038.
[27] Z. Hou, B. Lin, Y. Bao, H. ning Yan, M. Zhang, X. wei Chang, X. xin Zhang, Z. jie Wang, G. fei Wei, M. sheng Cheng, Y. Liu, C. Guo, Dual-tail approach to discovery of novel carbonic anhydrase IX inhibitors by simultaneously matching the hydrophobic and hydrophilic halves of the active site, Eur. J. Med. Chem. 132 (2017) 1–10, https://doi.org/10.1016/j.ejmech.2017.03.023.
[28] A. Bonardi, A. Nocentini, S. Bua, J. Combs, C. Lomelino, J. Andring, L. Lucarini, S. Sgambellone, E. Masini, R. McKenna, P. Gratteri, C.T. Supuran, Sulfonamide inhibitors of human carbonic anhydrases designed through a three-tails approach: improving ligand/isoform matching and selectivity of action, J. Med. Chem. 63 (2020) 7422–7444, https://doi.org/10.1021/acs.jmedchem.0c00733.
[29] M. Bozdag, M. Ferraroni, E. Nuti, D. Vullo, A. Rossello, F. Carta, A. Scozzafava, C.T. Supuran, Combining the tail and the ring approaches for obtaining potent and isoform-selective carbonic anhydrase inhibitors: solution and X-ray crystallographic studies, Bioorg. Med. Chem. 22 (2014) 334–340, https://doi.org/10.1016/j.bmc.2013.11.016.
[30] M.A. Pinard, B. Mahon, R. McKenna, Probing the surface of human carbonic anhydrase for clues towards the design of isoform specific inhibitors, Biomed. Res. Int. 2015 (2015), https://doi.org/10.1155/2015/453543.
[31] V. Alterio, A. Di Fiore, K. D'Ambrosio, C.T. Supuran, G. De Simone, Multiple binding modes of inhibitors to carbonic anhydrases: how to design specific drugs targeting 15 different isoforms? Chem. Rev. 112 (2012) 4421–4468, https://doi.org/10.1021/cr200176r.
[32] M. Krasavin, M. Korsakov, Z. Zvonaryova, E. Semyonychev, T. Tuccinardi, S. Kalinin, M. Tanç, C.T. Supuran, Human carbonic anhydrase inhibitory profile of mono- and bis-sulfonamides synthesized via a direct sulfochlorination of 3- and 4-(hetero)arylisoxazol-5-amine scaffolds, Bioorg. Med. Chem. 25 (2017) 1914–1925, https://doi.org/10.1016/j.bmc.2017.02.018.
[33] S. Kalinin, S. Kopylov, T. Tuccinardi, A. Sapegin, D. Dar'in, A. Angeli, C.T. Supuran, M. Krasavin, Lucky Switcheroo: dramatic potency and selectivity improvement of imidazoline inhibitors of human carbonic anhydrase VII, ACS Med. Chem. Lett. (2017), https://doi.org/10.1021/acsmedchemlett.7b00300.
[34] G. La Regina, A. Coluccia, V. Famiglini, S. Pelliccia, L. Monti, D. Vullo, E. Nuti, V. Alterio, G. De Simone, S.M. Monti, P. Pan, S. Parkkila, C.T. Supuran, A. Rossello, R. Silvestri, Discovery of 1,1′-biphenyl-4-sulfonamides as a new class of potent and selective carbonic anhydrase XIV inhibitors, J. Med. Chem. 58 (2015) 8564–8572, https://doi.org/10.1021/acs.jmedchem.5b01144.
[35] A study of SLC-0111 and Gemcitabine for Metastatic Pancreatic Ductal cancer in Subjects positive for CAIX - Full Text View - ClinicalTrials.gov, (n.d.). https://www.clinicaltrials.gov/ct2/show/NCT03450018?term=SLC-0111 (accessed 10.02.21).
[36] S. Durdagi, M. Entürk, D. Ekinci, H.T. Balaydin, S. Göksu, Ö.I. Küfreviolu, A. Innocenti, A. Scozzafava, C.T. Supuran, Kinetic and docking studies of phenol-based inhibitors of carbonic anhydrase isoforms I, II, IX and XII evidence a new binding mode within the enzyme active site, Bioorg. Med. Chem. 19 (2011) 1381–1389, https://doi.org/10.1016/j.bmc.2011.01.016.
[37] C. Chazalette, B. Masereel, S. Rolin, A. Thiry, A. Scozzafava, A. Innocenti, C.T. Supuran, Carbonic anhydrase inhibitors. Design of anticonvulsant sulfonamides incorporating indane moieties, Bioorg. Med. Chem. Lett 14 (2004) 5781–5786, https://doi.org/10.1016/j.bmcl.2004.09.061.
[38] S. Kalinin, A. Nocentini, A. Kovalenko, V. Sharoyko, A. Bonardi, A. Angeli, P. Gratteri, T.B. Tennikova, C.T. Supuran, M. Krasavin, From random to rational: a discovery approach to selective subnanomolar inhibitors of human carbonic anhydrase IV based on the Castagnoli-Cushman multicomponent reaction, Eur. J. Med. Chem. 182 (2019), https://doi.org/10.1016/j.ejmech.2019.111642.
[39] G. Poli, S. Galati, A. Martinelli, C.T. Supuran, T. Tuccinardi, Development of a cheminformatics platform for selectivity analyses of carbonic anhydrase inhibitors, J. Enzym. Inhib. Med. Chem. 35 (2020) 365–371, https://doi.org/10.1080/14756366.2019.1705291.
[40] S. Galati, D. Yonchev, R. Rodríguez-Pérez, M. Vogt, T. Tuccinardi, J. Bajorath, Predicting isoform-selective carbonic anhydrase inhibitors via machine learning and rationalizing structural features important for selectivity, ACS Omega (2021), https://doi.org/10.1021/acsomega.0c06153.
[41] C.T. Supuran, Advances in structure-based drug discovery of carbonic anhydrase inhibitors, Expet Opin. Drug Discov. 12 (2017) 61–88, https://doi.org/10.1080/17460441.2017.1253677.
[42] M. Krasavin, S. Kalinin, T. Sharonova, C.T. Supuran, Inhibitory activity against carbonic anhydrase IX and XII as a candidate selection criterion in the development of new anticancer agents, J. Enzym. Inhib. Med. Chem. 35 (2020) 1555–1561, https://doi.org/10.1080/14756366.2020.1801674.
[43] G. Karageorgis, S. Warriner, A. Nelson, Efficient discovery of bioactive scaffolds by activity-directed synthesis, Nat. Chem. 6 (2014) 872–876, https://doi.org/10.1038/nchem.2034.
[44] F.W. Bollinger, L.D. Tuma, Diazotransfer reagents 1, Synlett. 1996 (1996) 407–413, https://doi.org/10.1055/s-1996-5440.
[45] D. Dar'in, G. Kantin, M. Krasavin, A "sulfonyl-azide-free" (SAFE) aqueous-phase diazo transfer reaction for parallel and diversity-oriented synthesis, Chem. Commun. 55 (2019) 5239–5242, https://doi.org/10.1039/c9cc02042j.
[46] I. Shershnev, D. Dar'in, S. Chuprun, G. Kantin, O. Bakulina, M. Krasavin, The use of ∝-diazo-γ-butyrolactone in the Büchner-Curtius-Schlotterbeck reaction of cyclic ketones: a facile entry into spirocyclic scaffolds, Tetrahedron Lett. 60 (2019) 1800–1802, https://doi.org/10.1016/j.tetlet.2019.06.008.
[47] J. Synofzik, D. Dar'In, M.S. Novikov, G. Kantin, O. Bakulina, M. Krasavin, α-Acyl-α-diazoacetates in transition-metal-free β-lactam synthesis, J. Org. Chem. 84 (2019) 12101–12110, https://doi.org/10.1021/acs.joc.9b02030.
[48] M. Gecht, G. Kantin, D. Dar'in, M. Krasavin, A novel approach to biologically relevant oxazolo[5,4-d]pyrimidine-5,7-diones via readily available diazo-barbituric acid derivatives, Tetrahedron Lett. 60 (2019) 151120, https://doi.org/10.1016/j.tetlet.2019.151120.
[49] D. Dar'in, G. Kantin, O. Bakulina, M. Krasavin, Facile one-pot access to α-Diazo-β-ketosulfones from sulfonyl chlorides and α-haloketones, Synth. Met. 52 (2020) 2259–2266, https://doi.org/10.1055/s-0040-1707525.
[50] A. Bubyrev, D. Dar'in, G. Kantin, M. Krasavin, Synthetic studies towards CH-diazomethane sulfonamides: a novel type of diazo reagents, Eur. J. Org Chem. 2020 (2020) 4112–4115, https://doi.org/10.1002/ejoc.202000446.
[51] D. Zhukovsky, D. Dar'in, M. Krasavin, Rh2(esp)2-Catalyzed coupling of α-Diazo-γ-butyrolactams with aromatic amines, Eur. J. Org Chem. 2019 (2019) 4377–4383, https://doi.org/10.1002/ejoc.201900565.
[52] R.G. Khalifah, The carbon dioxide hydration activity of carbonic anhydrase, J. Biol. Chem. 246 (1971) 2561–2573. http://www.jbc.org/content/246/8/2561.
[53] S. Pastorekova, S. Parkkila, J. Pastorek, C.T. Supuran, Carbonic anhydrases: current state of the art, therapeutic applications and future prospects, J. Enzym. Inhib. Med. Chem. 19 (2004) 199–229, https://doi.org/10.1080/14756360410001689540.
[54] A. Angeli, F. Carta, A. Nocentini, J.-Y. Winum, R. Zalubovskis, A. Akdemir, V. Onnis, W.M. Eldehna, C. Capasso, G. De Simone, S.M. Monti, S. Carradori, W.A. Donald, S. Dedhar, C.T. Supuran, Carbonic anhydrase inhibitors targeting metabolism and tumor microenvironment, Metabolites 10 (2020) 412, https://doi.org/10.3390/metabo10100412.
[55] V. Burianova, S. Kalinin, C.T. Supuran, M. Krasavin, Radiotracers for positron emission tomography (PET) targeting tumour-associated carbonic anhydrase isoforms, Eur. J. Med. Chem. (2020), https://doi.org/10.1016/j.ejmech.2020.113046.
[56] S. Dong Soo, P. Won Young, K. Ki Hyung, K. Ahrong, K. Young Keum, K. Kyungbin, C. Kyung Un, Differential regulation and prognostic significance of endogenous hypoxic markers in endometrial carcinomas, Eur. J. Gynaecol. Oncol. 39 (2018) 773–778.
[57] C.T. Supuran, Therapeutic applications of the carbonic anhydrase inhibitors, Therapy 4 (2007) 355–378, https://doi.org/10.2217/14750708.4.3.355.
[58] B. Cvenkel, M. Kolko, Current medical therapy and future trends in the management of glaucoma treatment, J. Ophthalmol. 2020 (2020), https://doi.org/10.1155/2020/6138132.
[59] C.T. Supuran, V. Alterio, A. Di Fiore, K. D'Ambrosio, F. Carta, S.M. Monti, G. De Simone, Inhibition of carbonic anhydrase IX targets primary tumors, metastases, and cancer stem cells: three for the price of one, Med. Res. Rev. 38 (2018) 1799–1836, https://doi.org/10.1002/med.21497.
[60] P. Ebbesen, E.O. Pettersen, T.A. Gorr, G. Jobst, K. Williams, J. Kieninger, R.H. Wenger, S. Pastorekova, L. Dubois, P. Lambin, B.G. Wouters, T. Van Den Beucken, C.T. Supuran, L. Poellinger, P. Ratcliffe, A. Kanopka, A. Görlach, M. Gasmann, A.L. Harris, P. Maxwell, A. Scozzafava, Taking advantage of tumor cell adaptations to hypoxia for developing new tumor markers and treatment strategies, J. Enzym. Inhib. Med. Chem. 24 (2009) 1–39, https://doi.org/10.1080/14756360902784425.
[61] A. Waheed, W.S. Sly, Carbonic anhydrase XII functions in health and disease, Gene 623 (2017) 33–40, https://doi.org/10.1016/j.gene.2017.04.027.
[62] C.T. Supuran, Carbonic anhydrase inhibitors as emerging agents for the treatment and imaging of hypoxic tumors, Expet Opin. Invest. Drugs 27 (2018) 963–970, https://doi.org/10.1080/13543784.2018.1548608.
[63] R. Baghban, L. Roshangar, R. Jahanban-Esfahlan, K. Seidi, A. Ebrahimi-Kalan, M. Jaymand, S. Kolahian, T. Javaheri, P. Zare, Tumor microenvironment complexity and therapeutic implications at a glance, Cell Commun. Signal. 18 (2020), https://doi.org/10.1186/s12964-020-0530-4.
[64] S.H. Lee, J.R. Griffiths, How and why are cancers acidic? Carbonic anhydrase ix and the homeostatic control of tumour extracellular ph, Cancers (Basel) 12 (2020) 1–23, https://doi.org/10.3390/cancers12061616.
[65] H.M. Becker, Carbonic anhydrase IX and acid transport in cancer, Br. J. Canc. 122 (2020) 157–167, https://doi.org/10.1038/s41416-019-0642-z.
[66] S.H. Lee, D. McIntyre, D. Honess, A. Hulikova, J. Pacheco-Torres, S. Cerdán, P. Swietach, A.L. Harris, J.R. Griffiths, Carbonic anhydrase IX is a pH-stat that sets an acidic tumour extracellular pH in vivo, Br. J. Canc. 119 (2018) 622–630, https://doi.org/10.1038/s41416-018-0216-5.
[67] G. Ilardi, N. Zambrano, F. Merolla, M. Siano, S. Varricchio, M. Vecchione, G. Rosa, M. Mascolo, S. Staibano, Histopathological determinants of tumor resistance: a special look to the immunohistochemical expression of carbonic anhydrase IX in human cancers, Curr. Med. Chem. 21 (2014) 1569–1582, https://doi.org/10.2174/09298673113209990227.

[68] Inhibition of carbonic anhydrase in combination with Platinum and Etoposide-based Radiochemotherapy in patients with localized small cell lung cancer - Full Text View - ClinicalTrials.gov, (n.d.). https://clinicaltrials.gov/ct2/show/NCT03467360 (accessed February 10.02.21.).
[69] Trial to determine Optimal phase II dose of the oral dual CAIX inhibitor/radiosensitizer - Full Text View - ClinicalTrials.gov, (n.d.). https://clinicaltrials.gov/ct2/show/NCT02216669?term=carbonic+anhydrase&draw=4 (accessed 10.02.21.).
[70] C.Y. Chu, Y.T. Jin, W. Zhang, J. Yu, H.P. Yang, H.Y. Wang, Z.J. Zhang, X.P. Liu, Q. Zou, CA IX is upregulated in CoCl2-induced hypoxia and associated with cell invasive potential and a poor prognosis of breast cancer, Int. J. Oncol. 48 (2016) 271–280, https://doi.org/10.3892/ijo.2015.3253.
[71] W.M. Eldehna, A. Nocentini, S.T. Al-Rashood, G.S. Hassan, H.M. Alkahtani, A.A. Almehizia, A.M. Reda, H.A. Abdel-Aziz, C.T. Supuran, Tumor-associated carbonic anhydrase isoform IX and XII inhibitory properties of certain isatin-bearing sulfonamides endowed with in vitro antitumor activity towards colon cancer, Bioorg. Chem. 81 (2018) 425–432, https://doi.org/10.1016/j.bioorg.2018.09.007.
[72] H.I. Gul, C. Yamali, H. Sakagami, A. Angeli, J. Leitans, A. Kazaks, K. Tars, D.O. Ozgun, C.T. Supuran, New anticancer drug candidates sulfonamides as selective hCA IX or hCA XII inhibitors, Bioorg. Chem. 77 (2018) 411–419, https://doi.org/10.1016/j.bioorg.2018.01.021.
[73] M. Krasavin, R. Žalubovskis, A. Grandāne, I. Domračeva, P. Zhmurov, C.T. Supuran, Sulfocoumarins as dual inhibitors of human carbonic anhydrase isoforms IX/XII and of human thioredoxin reductase, J. Enzym. Inhib. Med. Chem. 35 (2020) 506–510, https://doi.org/10.1080/14756366.2020.1712596.
[74] M.A. Abdelrahman, W.M. Eldehna, A. Nocentini, S. Bua, S.T. Al-Rashood, G.S. Hassan, A. Bonardi, A.A. Almehizia, H.M. Alkahtani, A. Alharbi, P. Gratteri, C.T. Supuran, Novel diamide-based benzenesulfonamides as selective carbonic anhydrase ix inhibitors endowed with antitumor activity: synthesis, biological evaluation and in silico insights, Int. J. Mol. Sci. 20 (2019), https://doi.org/10.3390/ijms20102484.
[75] J.B. Baell, J.W.M. Nissink, Seven year itch: pan-assay interference compounds (PAINS) in 2017 - utility and limitations, ACS Chem. Biol. 13 (2018) 36–44, https://doi.org/10.1021/acschembio.7b00903.
[76] D. Zhukovsky, D. Dar'in, G. Kantin, M. Krasavin, Synthetic exploration of α-diazo γ-butyrolactams, Eur. J. Org. Chem. 2019 (2019) 2397–2400, https://doi.org/10.1002/ejoc.201900133.
[77] D. Dar'in, G. Kantin, M. Krasavin, Practical application of the aqueous "sulfonyl-azide-free" (SAFE) diazo transfer protocol to less α-C-H acidic ketones and esters, Synth. Met. 51 (2019) 4284–4290, https://doi.org/10.1055/s-0039-1690613.
[78] B.L. Wilkinson, L.F. Bornaghi, T.A. Houston, A. Innocente, C.T. Supuran, S.A. Poulsen, A novel class of carbonic anhydrase inhibitors: glycoconjugate benzene sulfonamides prepared by "click-tailing", J. Med. Chem. 49 (2006) 6539–6548, https://doi.org/10.1021/jm060967z.
[79] M. Lopez, A.J. Salmon, C.T. Supuran, S.-A. Poulsen, Carbonic anhydrase inhibitors developed through 'click tailing', Curr. Pharmaceut. Des. 16 (2010) 3277–3287, https://doi.org/10.2174/138161210793429869.
[80] B.L. Wilkinson, L.F. Bornaghi, T.A. Houston, A. Innocenti, D. Vullo, C.T. Supuran, S.A. Poulsen, Carbonic anhydrase inhibitors: inhibition of isozymes I, II, and IX with triazole-linked O-glycosides of benzene sulfonamides, J. Med. Chem. 50 (2007) 1651–1657, https://doi.org/10.1021/jm061320h.
[81] N. Pala, L. Micheletto, M. Sechi, M. Aggarwal, F. Carta, R. McKenna, C.T. Supuran, Carbonic anhydrase inhibition with benzenesulfonamides and tetrafluorobenzenesulfonamides obtained via click chemistry, ACS Med. Chem. Lett. 5 (2014) 927–930, https://doi.org/10.1021/ml500196t.